Analysis of *Aedes aegypti* microRNAs in response to *Wolbachia* *w*AlbB infection and their potential role in mosquito longevity

Cameron Bishop[1], Mazhar Hussain[1], Leon E. Hugo[2], Sassan Asgari[1]*

[1]Australian Infectious Disease Research Centre, School of Biological Sciences, The University of Queensland, Brisbane, QLD 4072, Australia

[2]Mosquito Control Laboratory, QIMR Berghofer Medical Research Institute, 300 Herston Road, Herston, 4006, Australia

Running title: Altered mosquito miRNAs upon *Wolbachia* infection

*Corresponding author: Sassan Asgari; Tel: +617 3365 2043; s.asgari@uq.edu.au

Abstract

The mosquito *Aedes aegypti* is the primary vector of a range of medically important viruses including dengue, Zika, West Nile, yellow fever, and chikungunya viruses. The endosymbiotic bacterium *Wolbachia pipientis w*AlbB strain has emerged as a promising biocontrol agent for blocking viral transmission by *Ae. aegypti*. In order to predict and manage the long-term efficacy of its application in the field, a thorough understanding of the molecular interactions between symbiont, host, and pathogen is required. *Wolbachia* are known to influence host physiology in a variety of ways including reproduction, innate immunity, metabolism, and longevity. MicroRNAs (miRNAs) are highly conserved small non-coding RNAs that are important regulators of gene expression in eukaryotes and viruses. A number of miRNAs have been functionally described in *Drosophila* and mosquitoes as having roles in regulating a broad range of biological processes, as well as facilitating *Wolbachia* maintenance. We generated the first chromosomal map of *Ae. aegypti* miRNAs, and compared the miRNA expression profiles between a *w*AlbB-transinfected *Ae. aegypti* mosquito line and a tetracycline cleared derivative using deep small RNA-sequencing. We found a number of miRNAs to be modulated by *w*AlbB infection. We also found that some miRNAs were upregulated with age in a manner that was affected by *w*AlbB. By selectively inhibiting some differentially expressed miRNAs, we identified miR-2946-3p and miR-317-3p as effecting mosquito longevity.

Importance

Wolbachia is an endosymbiotic bacterium found in about 65% of insect species. It is mostly known for reproductive manipulations of the host, and also blocking replication of negative sense RNA viruses. Transinfection of *Wolbachia* into *Aedes aegypti* mosquitoes, which transmit a variety of arboviruses, including dengue virus, has provided a novel biological approach in reducing transmission of arboviruses. To gain a better understanding of

Wolbachia-mosquito interactions, we investigated the impact of *Wolbachia* on the microRNA profile of *Ae. aegypti* mosquitoes. Besides identifying several differentially expressed microRNAs and their putative target genes, we found alterations of microRNAs in mosquitoes due to age. Inhibition of two miRNAs led to reduced mosquito life span. The outcomes provide insights into underlying molecular mechanisms involved in *Wolbachia*-host interactions.

Keywords: *Wolbachia*; mosquito; *Aedes aegypti*; *w*AlbB; microRNA

Introduction

Arthropod-borne viruses (arboviruses) pose a significant and increasing global health burden. Two mosquitoes of the *Aedes* genus, *Aedes aegypti* and *Aedes albopictus,* are the primary and secondary vectors, respectively, of several medically important arboviruses including the flaviviruses dengue virus (DENV), Zika virus (ZIKV), yellow fever virus (YFV), and the alphavirus chikungunya virus (CHIKV) (1, 2). Originating in sub-Saharan Africa, *Ae. aegypti* experienced a dramatic range expansion beginning with European colonisation of the Americas in the 16th century (3). Human activity has continued to facilitate its global spread, and today it is common in many urban subtropical and tropical habitats across six continents (4). In the absence of safe or effective vaccines, vector control remains the most effective method for limiting outbreaks of mosquito-borne viruses (5, 6). With many *Ae. aegypti* populations becoming resistant to insecticides, attention has turned to biological vector-control strategies (7-9).

The endosymbiotic bacterium *Wolbachia pipientis* has proven to be a useful biocontrol agent through its ability to invade mosquito populations and prevent viral transmission, either by suppressing the mosquito population or by inhibiting virus infection and dissemination within individual mosquitoes (10, 11). The ability for some strains of *Wolbachia* to invade mosquito populations is due to a combination of maternal inheritance and a manipulation by the

63 bacterium known as cytoplasmic incompatibility, which provides a reproductive advantage to
64 infected females in naïve or heterologously-infected populations (12, 13). Additional factors
65 governing the success of a *Wolbachia* invasion include the fitness cost to the mosquito
66 harbouring *Wolbachia*, and the ability of *Wolbachia* to tolerate the climate of tropical regions,
67 where mosquito-borne viruses primarily exist (14-16). The viral-inhibition phenotype
68 exhibited by some strains of *Wolbachia* is complex, not well-understood, and varies depending
69 on the combination of *Wolbachia* strain and mosquito host (17-19).
70 Several *Wolbachia* strains have been investigated for their efficacy in biocontrol, and to explore
71 the biology that underpins their association with the host. The *Drosophila*-derived *w*MelPop
72 and *w*Mel strains have been investigated in laboratory and/or field trials for suppression of
73 West Nile virus (WNV), YFV, ZIKV, DENV, and CHIKV in *Ae. aegypti*. Despite effectively
74 supressing viral infection and transmission (20-24), their ability to be maintained at high
75 frequency in wild populations is limited by the large fitness cost of *w*MelPop (14), and the
76 sensitivity to heat-stress of *w*Mel (25, 26). An *Ae. albopictus*-derived strain, *w*AlbB, inhibits
77 transmission of DENV in *Ae. aegypti*, while also being more tolerant of heat stress than *w*Mel
78 or *w*MelPop, allowing it to persist in wild populations (25, 27-30).
79 The symbiotic relationship between *Wolbachia* and host is intimate and complex, with each
80 party affecting the other through multiple physiological pathways, including innate immunity,
81 redox homeostasis, metabolism, protein synthesis and proteolysis, nutrient provisioning, and
82 iron homeostasis (19, 31-39). *Wolbachia* infection has also been shown to have a significant
83 effect on host gene expression via the microRNA (miRNA) pathway.
84 miRNAs are small non-coding RNAs involved in the regulation of gene expression in
85 eukaryotes and viruses (40). In mosquitoes, a number of miRNAs are conserved among
86 disparate lineages, indicating their importance in regulating critical functions. For example,
87 miR-281, miR-184, miR-989 and miR-278 are conserved among *Anopheles gambiae*, *Ae.*

88 *aegypti*, and *Culex quinquefasciatus* (41). Some conserved miRNAs also show conserved
89 patterns of expression among tissue types, or developmental stages, or in response to
90 physiological cues such as blood feeding, reproduction, or infection by pathogens (41, 42). In
91 *Ae. aegypti*, several miRNAs have been functionally explored. The ovary-specific miR-309 is
92 induced by blood feeding and has been shown to regulate ovarian development by targeting
93 the *SIX4* transcript (43). miR-1174 is involved in bloodmeal intake by targeting *serine*
94 *hydroxymethyltransferase*, while miR-1890 regulates blood digestion by targeting the *JHA15*
95 transcript (41, 44).
96 A number of miRNAs are modulated by arbovirus infection in *Ae. aegypti*, some of which have
97 been predicted to have an effect on viral replication (41, 45). For example, miR-2944b-5p is
98 exploited by CHIKV to enhance its replication via a direct interaction with the 3' UTR of the
99 viral genome, and indirectly via repression of a host target gene, vps-13 (46). Similarly, the
100 blood-meal induced miR-375 has been implicated in enhancing DENV-2 infection in *Ae.*
101 *aegypti* via the Toll pathway by inducing *cactus* and repressing *REL1* (47). In experiments
102 using *Ae. aegypti*, *Wolbachia w*MelPop induced the expression of miR-2940, which in turn
103 promoted the maintenance of *w*MelPop by supressing methyltransferase *Dnmt2*, and by
104 inducing arginine methyltransferase (48, 49). Furthermore, miR-2940 has been shown to
105 inhibit DENV and WNV infection in *Ae. aegypti* and *Ae. albopictus* via induction of the
106 metalloprotease m41 ftsh (48, 50). The miR-2940 instance provides an elegant example of
107 symbiosis between *Wolbachia* and *Ae. aegypti,* and underscores the importance of the miRNA
108 pathway in facilitating the interaction. It remains to be seen how the effect on host miRNA
109 profile imposed by *w*MelPop compares to that of *w*AlbB.
110 To further shed light on the role of miRNAs in mosquito-*Wolbachia* interactions, in the current
111 study, we used deep-sequencing of small RNAs to investigate the effect of *Wolbachia w*AlbB
112 strain on the miRNA expression profile of *Ae. aegypti* mosquitoes. By comparing *w*AlbB-

113 infected mosquitoes with a tetracycline-cleared line, we detected differential expression of
114 several miRNAs between lines, with some miRNAs differentially expressed with age. Further,
115 our results suggest that upregulation of aae-miR-2946-3p and aae-miR-317-3p could be related
116 to mosquito longevity in *w*AlbB-infected mosquitoes. A number of the differentially expressed
117 miRNAs have been described elsewhere as being involved in the regulation of metabolism,
118 microbial defence, reproduction, development and ageing in mosquitoes.

119 **Materials and Methods**

120 **Mosquitoes**

121 The *Wolbachia w*AlbB infected *Ae. aegypti* strain *w*AlbB2-F4 mosquitoes (51) were used for
122 experiments in this study. We call the strain WB2 for shortness. A *Wolbachia*-free (WB2.tet)
123 line was produced by feeding adults on 10% sucrose with 1mg/ml tetracycline hydrochloride
124 (Sigma) for seven generations. WB2.tet mosquitoes were maintained for five generations
125 without tetracycline before testing for the presence of *Wolbachia w*AlbB using qPCR on
126 genomic DNA with primers to the *Wolbachia surface protein* (*wsp*) gene from nine adult
127 females to ensure removal of *Wolbachia*. See qPCR below for primer sequences and details.
128 Female WB2 mosquitoes were also tested for *Wolbachia* density by the same method. Both
129 lines were reared by hatching 300 eggs in 27°C water and feeding larvae daily with ground
130 Tropical Colour flasks (Tetra) fish food *ad libitum.* Adults were maintained at 27°C, a
131 12hr:12hr day/night cycle with relative humidity ranging between 65-75%, and allowed to feed
132 *ad libitum* on 10% sucrose. All mosquito experiments were performed using female adults.

133 **Cell line**

134 The *Ae. aegypti* Aag2.*w*AlbB cell line was generated as described in (52) for testing the effect
135 of miRNA inhibition of aae-miR-2b-3p, aae-miR-190-5p, and aae-miR-276b-5p on *w*AlbB
136 density. Cells were maintained in a 1:1 ratio of Mitsuhashi-Maramorosch (Himedia) and

137 Schneider's Drosophila Medium (Invitrogen, Carlsbad, USA) supplemented with 10% Foetal
138 Bovine Serum (FBS) (Bovogen Biologicals, French origin) at 27°C as monolayer.

139 **Small RNA sequencing**

140 Adult female mosquitoes were sampled at 2, 6, and 12 days post emergence. Three replicate
141 pools of four females were sampled at each time point. Samples were homogenised in 1.5ml
142 tubes on ice using a plastic micro-pestle and small RNAs were extracted using the miRNeasy
143 Mini Kit (QIAGEN, Hilden, Germany). Genomic DNA was removed using the Turbo DNA-
144 free kit (Invitrogen) as per the manufacturer's instructions. Total RNA from each sample was
145 quantified and purity determined using an Agilent 2100 Bioanalyzer (Agilent Technologies,
146 Palo Alto, CA, USA), NanoDrop (Thermo Fisher Scientific Inc.) and performing gel
147 electrophoresis in a 1% agarose gel. The following steps relating to library preparation and
148 sequencing were carried out by the sequencing service company Genewiz (China). Two µg of
149 total RNA with RNA integrity number (RIN) value of above 7.5 was used for subsequent
150 library preparation. Indexed sequencing libraries were constructed according to the
151 manufacturer's protocol (NEBNext Multiplex Small RNA library Prep Set for Illumina). The
152 resulting PCR products of ~140 bp were recovered and purified via polyacrylamide agarose
153 gel electrophoresis, validated using an Agilent 2100 Bioanalyzer (Agilent Technologies), and
154 quantified using a Qubit 2.0 Fluorometer (Invitrogen). Libraries were then multiplexed and
155 sequenced on an Illumina HiSeq 2500 instrument using a 1x50 single-end configuration
156 according to manufacturer's instructions (Illumina, San Diego, CA, USA). Image analysis and
157 base calling were conducted using the HiSeq Control Software (HCS), Off-Line Basecaller
158 (OLB), and GAPipeline-1.6 (Illumina).

159 **Bioinformatics analyses**

160 Low quality reads and adapters were removed from raw small RNA sequence reads using
161 Trimmomatic. Cleaned reads were then size-selected for reads between 18-24nt using BBmap

162 (53). Quality control was performed using FastQC (54). Mature miRNA annotations were
163 generated with miRdeep2 v0.1.2 (55) using four concatenated read files (two WB2.tet and two
164 WB2 - SRR12893564, SRR12893577, SRR12893581, SRR12893570), a previously published
165 list of *Ae. aegypti* precursor miRNA sequences (42), and miRBase databases for *Ae. aegypti*,
166 *Anopheles gambiae*, and *Drosophila melanogaster* (56) as input. miRDeep2 output provides
167 genomic coordinates of precursor miRNA loci, but not their corresponding mature sequences,
168 so we determined the exact mature miRNA locations using BLAST (57), and cross referenced
169 the results with the precursor coordinates. This method also allowed -5p and -3p designation
170 to each mature sequence, which was not included in miRDeep2's output. To quantify miRNA
171 expression, reads were mapped to the three complete chromosomes of the *Aedes aegypti*
172 AaegL5.0 reference genome (58) using Shortstack v3.8.5 (59) with default settings. Reads
173 mapping to mature miRNA annotations were counted using Shortstack with default settings. A
174 differential expression analysis was performed using EdgeR v3.34.0 (60). Low-count miRNAs
175 were removed using a minimum cutoff of 5 counts per million. Read counts were normalised
176 for library depth and composition using the trimmed mean of M-values method (61). Genewise
177 dispersion was modelled with the 'robust=T' parameter and the 'glmFit' function, and a test
178 for differential expression was performed using the 'glmLRT' function. For contrasts between
179 lines, miRNAs with a Benjamini & Hochberg adjusted p value of < 0.05 and a $\log_2$ fold-change
180 > 0.5 were considered differentially expressed. For contrasts between ages, miRNAs with an
181 adjusted p value of < 0.05 and a $\log_2$ fold-change of > 1 were considered differentially
182 expressed. The decision to relax the $\log_2$ fold-change cut-off to 0.5 for contrasts between lines
183 was based on the relatively low fold-changes observed in these contrasts compared to those in
184 contrasts between ages. Positive $\log_2$ fold-changes indicate a higher expression level in the
185 *w*AlbB-infected mosquitoes versus control. To assess the microbiome of each mosquito line,

186 unmapped reads were analysed using Kraken with the minikraken2 database (62). All data
187 were plotted using Kronatools (63) and R v3.6.3.
188 To predict gene targets of differentially expressed miRNAs, coding regions and 5'- and 3'-
189 UTRs of the AaegL5.0 transcriptome were scanned for potential binding sites using three
190 software packages: miRanda v3.3 (64), RNA22 v2.0 (65), and PITA v6.0 (66). We then took
191 target genes predicted by all three packages and performed a gene ontology term enrichment
192 analysis using VectorBase (67), with a *p* value cut-off of 0.05.
193 To identify putative hairpin structures expressed by *w*AlbB, WB2 fastq files were concatenated
194 within each age group. Reads of between 18 and 24 nt in length were mapped to the *Wolbachia*
195 *pipientis w*AlbB reference genome (Genbank Accession: NZ_CP031221.1) using (68) with
196 bowtie2 v2.2.7 (69). Peaks of high coverage were identified (≥ 2000 reads) using bedtools
197 v2.26.0 (70). High coverage peaks were visually examined using Integrated Genome Viewer
198 v2.11.9. RNA secondary structure was predicted using the The ViennaRNA Package (71).
199 Sequence alignment was performed using BioEdit v7.2 with the 'sliding ends' option.

200 **qPCR and RT-qPCR analysis**

201 Genomic DNA was extracted from 3 pools of 4 adult females at 2, 6, and 12 days post-
202 emergence using Econospin columns (Epoch Life Sciences), following a protocol described
203 previously (72). DNA was quantified using a BioTek Epoch Microspot plate
204 spectrophotometer. Quantitative PCR was performed using SYBR master mix (QIAGEN) in a
205 QIAGEN Rotor-Gene Q 2plex using 100ng of gDNA as per the manufacturer's instructions.
206 The ratio of *Wolbachia* to host genome copies was quantified by qPCR using previously
207 developed primers for the *Wolbachia* surface protein (*wsp*) gene and the *Ae. aegypti* Ribosomal
208 protein subunit 17 (*RPS17*) gene (21) (Table S1).
209 Total RNA was extracted from three pools of four adult females at 2, 6, and 12 days post-
210 emergence using the Qiazol reagent according to the manufacturer's instructions (Qiagen).

211 Genomic DNA was removed using the Turbo DNA-free kit (Invitrogen). RNA quality and
212 quantity were evaluated using a BioTek Epoch Microspot plate spectrophotometer. Small
213 RNAs were reverse transcribed with miSCRIPT II RT kit (QIAGEN) using the HiSpec buffer
214 and 0.5 µg of total RNA per reaction. Thermocycling conditions were as per the manufacturer's
215 instructions. The miSCRIPT RT kit works by poly-adenylating small RNA species present in
216 total RNA. A poly-T primer with a 5' universal tag is then used for reverse transcription of the
217 small RNAs. Quantitative PCR was performed with a miScript SYBR Green PCR kit
218 (QIAGEN) in a QIAGEN Rotor-Gene Q 2plex using 10 ng of cDNA per reaction. For each
219 small miRNA or 5s rRNA, the small RNA sequence was used for the forward primer sequence
220 (Table S1). The miScript Universal Primer (Qiagen) was used as the reverse primer.

221 **miRNA inhibitor trials**

222 Aag2.*w*AlbB cells were seeded into 12-well plates at a density of $5x10^5$ cells per well, and
223 allowed to adhere. Medium was removed and replaced with a 300µl of serum-free medium
224 containing 100nmol of miRNA inhibitor (GenePharma) in Cellfectin II reagent (Invitrogen).
225 miRNA inhibitors are RNA oligos, chemically modified to bind with high affinity to target
226 miRNAs. Target specificity derives from sequence complementarity, which is 100%.
227 Following incubation at 28˚C for three hours, 300µl of medium containing 2% FBS was added
228 to cells. Cells were then grown under normal culturing conditions for three days. DNA and
229 RNA were extracted and used for measuring *w*AlbB density and miRNA inhibition by qPCR
230 and miScript RT-qPCR, respectively, as described above. The effect of inhibition of aae-miR-
231 2b-3p, aae-miR-190-5p, and aae-miR-276b-5p on *w*AlbB density was examined *in vivo* by
232 intrathoracic microinjection of adult females with 125nl of 100µM inhibitor (GenePharma) or
233 a scrambled negative control at 2 days post emergence. As an additional control, mosquitoes
234 were injected with 125nl of phosphate-buffered saline (PBS). Three days after injection, DNA

235 and RNA were extracted and used for measuring *w*AlbB density and miRNA inhibition
236 respectively.
237 The effect of inhibition of aae-miR-317-3p and aae-miR-2946-3p on mosquito longevity was
238 performed by intrathoracic microinjection of adult females with 125nl of 100µM inhibitor,
239 (GenePharma) or a scrambled negative control (Table S1), or PBS at 2 days post emergence.
240 Mosquitoes that survived the 24-hour period following injection were included in the
241 experiment. Three days after injection, inhibition was measured by miScript qPCR as described
242 above. The experiment was performed twice, with 10 to 12 mosquitoes per treatment, per
243 experiment. Data were tested for proportionality using the cox.zph function in R, and analysed
244 using a Cox proportional hazards model, for the effect of treatment while controlling for batch
245 effect, using the survminer package in R. Tests returning a likelihood ratio test p value < 0.05
246 were considered significant. A Kaplan-Meier estimator was used to calculate median survival
247 estimates for each group.

248 **Quantification and statistical analysis**

249 All statistics were performed in R (version v3.6.2) or GraphPad Prism v. 9.1.2. Significance
250 for differences between treatment and control groups were determined by statistical analyses
251 mentioned in each relevant figure legend.

252 **Data and code availability**

253 The accession number for the small RNA-Seq dataset reported in this paper is SRA:
254 PRJNA671731 (will be released upon official acceptance).

255 **Results**

256 **Mosquito rearing and tetracycline clearance**

257 To produce a *Wolbachia*-free line as control, *w*AlbB-transinfected *Ae. aegypti* *w*AlbB2-F4
258 (WB2) mosquitoes (males and females) were treated with tetracycline (WB2.tet). We
259 confirmed the presence or absence of *Wolbachia* *w*AlbB in mosquitoes using qPCR of genomic

260 DNA from a sample of female mosquitoes in three age groups: 2, 6 and 12 days post-
261 emergence. No *Wolbachia* surface protein gene (WSP) product was detected in female WB2.tet
262 mosquitoes. In female WB2 mosquitoes, *w*AlbB density was not significantly different
263 between age groups (ANOVA, $p > 0.05$) (Fig. 1A).

264 **Small RNA sequencing**

265 To compare the miRNA profiles of WB2 and WB2.tet mosquitoes, we collected mosquitoes at
266 2, 6 and 12 dpe, from which RNA was extracted for RNA sequencing (RNA-Seq). Small RNA
267 sequencing of 18 RNA libraries yielded a total of 94.8 million single-end reads with a Phred
268 score of ≥Q30 after quality trimming and size selection (Table S2). After removing sequencing
269 adapters, the read length profile of each library was characteristic of a small RNA fraction,
270 with a sharp peak at 21-23nt corresponding to miRNA and short interfering-RNA classes, and
271 a broader peak at 26-31nt corresponding to PIWI-RNAs (Fig. S1). Reads of 18-24nt in length
272 were aligned to the *Ae. aegypti* AaegL5.0 genome, with an alignment rate of between 91.8%
273 and 96.5% per sample (Table S2). The total number of aligned 18-24nt reads ranged from 3.4
274 to 6.6×10^6 reads per sample (Fig. 1B). Following tetracycline treatment, each mosquito line
275 was reared under identical conditions for five generations. Nonetheless, to ensure that the
276 bacterial composition of each line was consistent, we conducted a metagenomics analysis using
277 reads that did not align to the AaegL5.0 genome. This confirmed that the bacterial composition
278 was congruent between lines (Fig. S2). To confirm the absence of *w*AlbB from the WB2.tet
279 samples, reads that did not map to the AaegL5.0 genome were mapped to the *w*AlbB genome.
280 For the *w*AlbB libraries, 3.42% of the reads mapped to the *w*AlbB genome, whereas for the
281 WB2.tet samples, 0.01% mapped, mainly to the 16s and 23s rRNA loci (Fig. 1C). To determine
282 the validity of these mappings, we collected the *w*AlbB-mapped WB2.tet reads and mapped
283 them against the genomes of five bacterial strains that were identified to the genus level in the
284 metagenomic analysis. Of those reads, 68.19% mapped to at least one of the five strains, mainly

285 to the rRNA loci. We therefore concluded that the small fraction of WB2.tet reads mapping to
286 the *w*AlbB genome was likely the result of sequence similarity between bacterial genomes, the
287 intrinsic error-rate associated with mapping short reads with a high sensitivity mapping
288 algorithm, and/or the result of index-hopping during library preparation.

289 **Annotation and differential expression analysis**

290 Previous annotations of precursor and mature miRNAs in *Ae. aegypti* relied on the scaffold-
291 level AaegL3.0 reference genome that is now superseded (73). We annotated miRNAs using
292 the current AaegL5.0 genome, which contains all three complete-length chromosome
293 assemblies and 2309 scaffolds (58). As a result of the improved completeness of the reference
294 genome, 13 miRNAs that were previously reported to be duplicated (42) were shown to occur
295 as single copies in the full-length chromosome assemblies and to be absent from the scaffolds.
296 A BLAST analysis of our miRNA sequences indicated that nine other miRNAs had potential
297 duplicates on a scaffold. The AaegL5.0 genome was produced from a pool of 80 individuals,
298 and many of the scaffolds are haplotigs, i.e. the result of alternative haplotypes present in the
299 pool (58). To confirm the validity of the duplicates, we aligned the chromosome copy and
300 scaffold copy of each potential duplicate, including 500b up- and downstream flanking regions.
301 All nine 'chromosome' copies had >95% similarity with their respective 'scaffold' copy across
302 the ~1100b alignment. We therefore assumed that the scaffolds on which those nine duplicates
303 occurred were haplotigs, and the duplicates were artificial. Since no unique miRNAs were
304 found on a scaffold, we removed the scaffolds from our analyses. Genomic coordinates for 221
305 mature and 116 precursor miRNA loci within the three full chomosomes of the AaegL5.0
306 genome are provided in Table S3. By comparing our annotations to the AaegL5.0 genome, we
307 determined the genomic context of each miRNA locus with respect to being intergenic,
308 intronic, or exonic, as well as identifying potential miRNA clusters (Fig. 2).

309 miRNAs with expression values greater than five counts-per-million in at least three samples
310 were included in the statistical analysis, resulting in 168 mature miRNAs being examined. A
311 principal components analysis of log_2 normalised counts showed clear separation of WB2 and
312 WB2.tet in each of the three age groups (Fig. 3A). In the 2 dpe group, differential expression
313 was approximately even in terms of up- vs down-regulation, whereas for 6 dpe and 12 dpe
314 groups, there was a skew toward downregulation (Fig. 3B). miRNAs with an adjusted p value
315 of < 0.05 and an absolute log_2 fold-change of > 0.5 were considered differentially expressed.
316 A total of 44 miRNAs met these criteria (Table 1). Log_2 fold-changes ranged from -2.05 to
317 1.57 (Table 1). There was minimal overlap in miRNAs that showed differential expression
318 between lines (Fig. 3C). Two miRNAs, aae-miR-12-5p and aae-miR-998-5p, were consistently
319 differentially expressed in both 2 dpe and 6 dpe groups (Table 1). A third miRNA, aae-miR-
320 309a-3p, was upregulated at 2 dpe and downregulated at 12 dpe (Table 1). No miRNAs were
321 significantly differentially expressed across all three age groups. Given the apparent lack of
322 consistency between age groups, we compared log_2 fold-changes of miRNAs that were
323 significantly differentially expressed in one age group against log_2 fold-changes of the same
324 miRNAs in other age groups - most of which were not significantly differentially expressed in
325 the second age group. All comparisons showed significant correlation, suggesting that despite
326 a lack of overlap between ages in terms of which miRNAs significantly changed abundance,
327 the broader expression pattern was generally consistent between age groups (Fig. 3D).
328 To validate differential expression of miRNAs between lines, we used a new generation of
329 mosquitoes and RT-qPCR to test ten miRNAs that showed relatively high log_2 fold-changes in
330 the original small RNA-Seq analysis (Table S4). One miRNA was too lowly expressed in
331 whole mosquitoes to amplify sufficiently via RT-qPCR, and was therefore excluded from
332 analysis. Seven miRNAs showed a trend that was consistent with that of the small RNA-Seq
333 results in at least two out of three age groups; of these, six were significantly differentially

334 expressed in the same age group that gave significant trends by small RNA-Seq (190-5p, 276b-
335 5p, 2940-5p, 2941-1-3p, 2946-3p, 309a-3p, and 31-3p 2dpe) (Fig. 4). A further two miRNAs
336 (308-5p, and 184-3p) showed a direction of change that was inconsistent with small RNA-Seq
337 (Fig. 4).
338 We next investigated the effect of age on miRNA expression. Generally, there was greater
339 differential expression between age groups than between lines (Fig. 3A), therefore, for
340 classifying miRNAs as being differentially expressed, we retained the FDR < 0.05 criterion,
341 but increased the $\log_2$ fold-change threshold from > 0.5 to > 1. A total of 34 miRNAs met these
342 criteria (Table 2). Of these, 14 showed age-related differential expression in both lines (2940-
343 5p, 34-5p, 317-3p, 11894b-3p, 11894a-4-3p, 11899-5p, 2946-3p, 1-5p, 1890-3p, 2765-5p,
344 309a-3p, 193-5p, 2765-5p, and 193-5p) (Fig. 5A, Table 2). Log_2 fold-changes ranged from -
345 2.61 to 1.56 in WB2.tet groups, and -2.70 to 3.47 in WB2 groups (Table 2). A total of 15
346 miRNAs that were differentially expressed with age were also differentially expressed between
347 lines (277-3p, 2941-1-3p, 2941-2-3p, 2946-3p, 2765-5p, 309a-3p, 286b-3p, 193-3p, 2942-3p,
348 279-3p, 996-3p, 276b-5p, 2941-1-5p, 196-3p, and 989-5p) (Table 1 and 2).
349 To validate differential expression of miRNAs between age groups, we used a new generation
350 of mosquitoes and RT-qPCR to test ten miRNAs that showed relatively high $\log_2$ fold-changes
351 and/or showed differential expression in both lines in the original sRNA-Seq (Table S4). Four
352 miRNAs were too lowly expressed in whole mosquitoes to amplify sufficiently via RT-qPCR,
353 and were therefore excluded from analysis. Of the six remaining miRNAs, five were
354 significantly upregulated with age (ANOVA, $p < 0.05$) (Fig. 5B). miR-2941-1-3p and 2940-5p
355 were both significantly different between lines, while 2946-3p and 2940-5p both indicated a
356 significant interaction between age and line (ANOVA, $p < 0.05$) (Fig. 5B). All miRNAs were
357 initially lower in WB2 than in WB2.tet, but increased at a greater rate to become even with or

358 higher than WB2.tet (Fig. 5B). miR-2940 showed differential expression with age in WB2
359 mosquitoes, but not in WB2.tet (Fig. 5B).

360 **Target prediction of differentially expressed miRNAs**

361 To determine if the expression of the predicted targets of the differentially expressed miRNAs
362 could be affected by age, we selected three highly confident targets of aae-miR-317-3p, and
363 aae-miR-2946-3p (Table 3). RNA extracted from WB2 and WB2.tet mosquitoes collected at
364 2, 6, and 12 dpe was subjected to RT-qPCR. aae-miR-317-3p and aae-miR-2946-3p were
365 upregulated in mosquitoes with age. RT-qPCR results revealed differential expression of most
366 of the predicted target genes of the two miRNAs with age (Fig. 6). For the targets of 317-3p,
367 AAEL010793 and AAEL010508 were significantly downregulated at 6 and 12 dpe compared
368 to 2 dpe, while the transcript levels of AAEL006171 steadily increased over time (Fig. 6). For
369 2946-3p targets, AAEL006095 did not change over time, AAEL006113 declined at 6 dpe but
370 increased at 12 dpe, and AAEL003402 significantly increased at 6 dpe but returned to the same
371 levels as those of 2 dpe at 12 dpe (Fig. 6). Overall, these results showed that the predicted
372 targets of the differentially expressed miRNAs also responded to age. However, these results
373 are only correlational and direct regulation/interaction of the miRNA-target combinations need
374 to be experimentally validated.

375 **Functional analysis of differentially expressed miRNAs**

376 We tested the effect of miRNA inhibition on *w*AlbB density in a transinfected Aag2.*w*AlbB
377 cell line by inhibiting two miRNAs, aae-miR-190-5p, and aae-miR-276b-5p, that were among
378 the most consistently upregulated in the WB2 versus WB2.tet mosquitoes according to small
379 RNA-Seq and RT-qPCR. Inhibition was done by transfecting the specific inhibitors (reverse
380 complementary short RNAs) of the miRNAs into Aag2.*w*AlbB cells, and was validated by RT-

381 qPCR three days after transfection. No increase in density was observed in the aae-miR-190-
382 5p, or aae-miR-276b-5p inhibited cells (Fig. 7).
383 We carried out a small-scale test of the effect of miRNA inhibition on the longevity of WB2
384 female mosquitoes by inhibiting two miRNAs, miR-317-3p, and miR-2946-3p, that were found
385 to increase with age to a greater degree in WB2 mosquitoes compared to WB2.tet. Three days
386 after miRNA inhibition, miR-317-3p and miR-2946-3p levels were significantly lower
387 (ANOVA, Tukey's HSD, $p < 0.001$) (Figs. 8A-D). Inhibition did not significantly affect
388 longevity in WB2.tet mosquitoes relative to controls, but in WB2 mosquitoes a significant
389 decrease in longevity was observed in response to inhibition of miR-2946-3p and miR-317-3p
390 compared to negative control (Cox proportional hazard, $p < 0.0001$, and $p = 0.130$,
391 respectively) (Figs. 8E & F). Following injection, the median survival according to a Kaplan-
392 Meier estimator was 26.5 days for miR-2946-3p-inhibited mosquitoes and 35.5 days for the
393 miR-317-3p-inhibited group. A survival estimate was not obtained for the NC and PBS control
394 groups, as not enough deaths occurred within the 40-day period. Longevity between PBS-
395 control mosquitoes did not differ significantly between WB2.tet and WB2 mosquitoes.

396 **Small RNA-Seq reads originating from *w*AlbB**

397 For each age group, WB2 small RNA-Seq read files were concatenated to produce a single
398 read file for each age group. These were filtered on the basis of read length so that only reads
399 18-24 nt long were retained. Reads were then aligned to the *w*AlbB reference genome, resulting
400 in 769,088, 691,639, and 748,995 aligned reads for 2 dpe, 6 dpe, and 12 dpe groups,
401 respectively. A total of 18 regions of high coverage (greater than 2000×) were identified, with
402 most being present in more than one age group (Table S5). Ten peaks corresponded to protein-
403 coding regions, four to intergenic regions, two to tRNAs, one peak corresponded to 5S rRNA,
404 and one to a pseudogene (Table S5). Two intergenic regions showed a pattern of read-coverage
405 reminiscent of precursor miRNA loci, and were predicted to form stem-loop structures (Figs.

406 S3-5A). Read-depth of these regions ranged from 3,200 to 16,000× per age group for the
407 concatenated read-files (Figs. S3 and S4). Small-RNA molecules are known to be produced by
408 *w*MelPop-CLA *Wolbachia* (74). Sequence alignment of those reported previously (74) and the
409 predicted stem-loop structures reported herein showed low sequence similarity (Fig. S5B). As
410 a control, we concatenated all three replicate fastq files from WB2.tet 2 dpe and mapped reads
411 to the *w*AlbB genome, then counted reads aligned to peaks 1 and 9 that form stem-loop
412 structures found in the WB2 samples. We found only three reads that mapped to peak 1
413 (compared to ~10,000 reads mapped in the WB2 samples) and no reads mapped to peak 9.

414 **Discussion**

415 Using deep sequencing of small RNAs, we identified 116 precursor and 221 mature *Ae. aegypti*
416 miRNA loci, and provide the first chromosomal mapping of these miRNAs. We detected
417 significant differential expression of 44 mature miRNAs in response to a persistent *w*AlbB-
418 infection in WB2 mosquitoes. We also report significant differential expression of 34 mature
419 miRNAs in response to ageing, 15 of which were also differentially expressed between the
420 *w*AlbB infected and uninfected lines.

421 There was limited overlap between age groups in terms of significant differential expression
422 of miRNAs in response to *w*AlbB. However, when miRNAs that were significantly
423 differentially expressed in one group were compared to the same miRNAs in other groups, they
424 showed significant positive correlation in $\log_2$ fold-change. This suggested that age groups did
425 show some degree of consistency in terms of differential expression due to *w*AlbB infection,
426 but not enough to be detectable by considering only miRNAs that gained significance in
427 EdgeR. The lack of overlap in significant differential expression could be due to a combination
428 of small sample size, unequal variances between groups, and the relatively weak effect of
429 *w*AlbB on miRNA expression. The effect of age, however, was more robust, and showed
430 reasonable concordance between lines.

431 We validated the small RNA-Seq results using RT-qPCR by assessing nine *w*AlbB-modulated,
432 and six age-modulated miRNAs that showed relatively high differential expression in small
433 RNA-Seq. For *w*AlbB-modulated miRNAs, the degree of concordance between small RNA-
434 Seq and RT-qPCR was satisfactory, with seven of the nine miRNAs showing agreement
435 between the two methods in at least two age groups. Of the ten age-modulated miRNAs that
436 we tried to validate, four were too lowly expressed in whole mosquitoes to allow sufficient
437 amplification by RT-qPCR. These were all miRNAs that were downregulated with age in the
438 small RNA-Seq analysis (1-5p, 193-5p, 2765-5p, and 2942-3p). Conversely, five of the six
439 validated miRNAs that significantly increased with age were among the most highly expressed
440 in our libraries (34-5p, 317-3p, 2941-1-3p, 2940-5p, and 2946-3p). Another feature of the age-
441 induced miRNAs was that the effect of age was more pronounced in the WB2 mosquitoes.
442 Expression of these miRNAs in the WB2 line was significantly lower compared to WB2.tet at
443 2 dpe for five of the six miRNAs validated by RT-qPCR. Expression in WB2 then increased
444 more dramatically than in WB2.tet, so that by 6 dpe and 12 dpe expression was the same or
445 higher in WB2 mosquitoes. The miR-2940-5p expression pattern was different; there was a
446 significant peak of expression in WB2 mosquitoes at 6 dpe followed by a drop at 12 dpe,
447 whereas in WB2.tet, expression did not change with age.
448 Some miRNAs form clusters in which individual hairpins are co-transcribed (75). The *Ae.*
449 *aegypti* genome contains a number of conserved miRNA clusters. One example is the miR-
450 2941-1/2941-2/2946 cluster, located in an intron of the putative transcription factor
451 AAEL009263 (14). The cluster is synapomorphic to *Aedes* mosquitoes, occurring in both *Ae.*
452 *aegypti* and *Ae. albopictus*, but absent from other *Culicids* and *Anophelines* (14, 76). Our RT-
453 qPCR results for miR-2941-1-3p and miR-2946-3p suggested co-transcription of the two
454 miRNA, with their dramatic suppression in *w*AlbB-infected mosquitoes at 2 dpe, and consistent
455 increase with age. The seed regions of miR-2941-1-3p and miR-2946-3p are identical, while

456 outside of the seed region, nucleotide identity is 25%. Both miR-2941-1-3p and miR-2946-3p
457 are involved in embryonic development in *Ae. aegypti* and *Ae. albopictus* (76, 77), and have
458 been observed to increase in response to *w*MelPop infection in *Ae. aegypti* cells (78).
459 miR-34-5p and miR-317-3p belong to the miR-317/277/34 cluster and both increased in
460 abundance with age, which is consistent with reports in *Drosophila* (79). miR-277 did not
461 increase with age in either line, which is also consistent with previous observations, and
462 possibly due to a reduced efficiency in the processing of miR-277 by the microprocessor
463 complex (79). In *Drosophila*, expression of the 317/277/34 cluster is known to be controlled
464 by the steroid hormone ecdysone (79). miR-34-5p has been shown to affect lifespan in flies by
465 modulating branched-chain amino acid catabolism (80), and the ecdysone signalling pathway
466 via downregulation of the *E74A* isoform of the transcription factor *Eip74EF* (79-81).
467 Furthermore, loss of function mutation in miR-34 causes dramatic life-shortening and
468 neurodegeneration in *Drosophila* (81). miR-34 and miR-277 are also involved in innate
469 immunity by regulating Toll signalling in *Drosophila*, with miR-34 promoting Toll signalling
470 and miR-277 having an inhibitory effect (82). In *Anopheline* mosquitoes, miR-34 is induced
471 by *Plasmodium* infection, and in *Ae. aegypti* Aag2 cells it is repressed by *w*MelPop infection
472 (78, 83).
473 In addition to the miR-2941-1/2941-2/2946 and miR-317/277/34 clusters, *w*MelPop has been
474 shown to modulate several other miRNAs that were differentially expressed in our WB2
475 mosquitoes. Our data showed upregulation of miR-190-5p in the WB2 line. In contrast,
476 *w*MelPop was reported to suppress miR-190 in cytoplasmic fractions of *Ae. aegypti* cells (78).
477 miR-190 has also been reported to be upregulated in response to CHIKV infection in *Ae.*
478 *albopictus* (41). The ovary-specific miR-309a-3p controls ovarian development and is
479 upregulated by *w*MelPop in *Ae. aegypti* mosquitoes (43, 84). We observed an initial

480 suppression of miR-309a-3p in WB2 mosquitoes at 2 dpe, then an upregulation at 6 dpe and
481 12 dpe, as well as a consistent increase with age in both lines, most strikingly in WB2.
482 Some differentially expressed miRNAs reported here showed a consistent trend of expression
483 in response to *w*AlbB across all age groups, while for others the effect was dependant on age.
484 Our data also showed that some previously documented age-related miRNAs increased
485 significantly with age in a manner that was affected by *w*AlbB infection. This raises the
486 question of whether *w*AlbB affects the longevity of *Ae. aegypti* via modulation of certain
487 miRNAs. In its native host *Ae. albopictus*, *w*AlbB has been found to decrease longevity in
488 males, but not in females (85). In *Ae. aegypti*, the results are less clear. In one study *w*AlbB-
489 infected females exhibited reduced longevity compared to uninfected controls (15). However,
490 it is reported elsewhere that *w*AlbB increased longevity following blood feeding (28). We
491 investigated the effect of two miRNAs; miR-317-3p and miR-2946-3p, that were significantly
492 upregulated with age and between lines, being higher in WB2 than WB2.tet. Neither miRNA
493 had an effect on longevity in WB2.tet mosquitoes, whereas in WB2 mosquitoes, inhibition was
494 associated with decreased survival. Further, when we compared longevity between WB2.tet
495 and WB2 control groups there was no difference. We hypothesise that the increase in miR-
496 2946-3p and miR-317-3p that we observed with age may form part of a response by *Ae. aegypti*
497 that offsets the fitness cost imposed by *w*AlbB; although to make a more concrete conclusion
498 on the effect of the miRNAs on longevity, this experiment needs to be repeated with larger
499 cohorts of mosquitoes. Additionally, it is possible that the combined stress of *Wolbachia*
500 infection together with the inhibition of any miRNA that is expressed during the adult life span
501 could affect survival. Therefore, to demonstrate a specific role for miR-2946-3p and miR-317-
502 3p in longevity of *w*AlbB-infected mosquitoes, inhibition of additional miRNAs that do not
503 show differential expression with age will be necessary. We found that the expression levels
504 of a number of the selected predicted targets miR-2946-3p, and miR-317-3p changed due to

505 age. However, further validation of direct interactions of these targets with the corresponding
506 miRNAs needs to be performed.
507 Previous studies have not found significant changes in the abundances of miRNAs between
508 *Wolbachia w*Mel-infected and uninfected *Drosophila* and mosquito cell lines (86) (87) or in
509 live flies (88). In *Ae. aegypti* Aag2-*w*Mel cells, RT-qPCR was used to assess the abundances
510 of 29 miRNAs that either had been shown in other studies to change in abundance upon
511 *Wolbachia* infection or had potential targets to bind to the 5' or 3' ends of the DENV genome
512 (86). No statistically significant changes were observed in the abundances of those miRNAs.
513 Of note, the investigators utilised *RPS17* as a normalizing gene, rather than small RNAs (such
514 as U6 or 5S) usually used for miRNA normalization in RT-qPCR. In *D. melanogaster* JW18
515 cells, also infected with *w*Mel strain, no significant alteration in miRNAs were observed
516 compared to control JW18Free cells analysed by small RNA-Seq (87). In *D. melanogaster* flies
517 infected with *w*Mel strain, no change was found in the abundances of 17 highly abundant
518 miRNAs assessed by RT-qPCR (88). In contrast, our previous study using microarray on *Ae.*
519 *aegypti* mosquitoes infected with *w*MelPop (84) and this study (*w*AlbB) using RNA-Seq
520 demonstrate changes in the abundances of a number of miRNAs in mosquitoes infected with
521 *Wolbachia*. The alterations were more pronounced in the case of *w*MelPop strain, which could
522 be related to its more pathogenic nature. The reason for the differences between our
523 observations with the other studies could be due to a number of factors. Firstly, the usage of
524 insects in our studies compared to cell lines in two of the abovementioned studies. It is known
525 that miRNAs show tissue specific expression and may respond differently in different tissues
526 to a stimulus. For example, in the case of aae-miR-2940-5p, the difference in the abundance of
527 the miRNA due to *Wolbachia w*MelPop infection is more pronounced in the midgut and fat
528 body tissues compared to ovary and salivary glands (89). Another factor could be strain-
529 specific effects of *Wolbachia* on the host and strain-host combinations that are different

530 between the studies. Further, in two of the studies (86, 87), a subset of selected miRNAs was
531 assessed rather than all miRNAs using high-throughput approaches such as microarray or
532 RNA-Seq.
533 The *w*MelPop-CLA strain of *Wolbachia* has been shown to regulate the expression of host and
534 *Wolbachia* genes via the production of small RNAs (74). Furthermore, sequence homology of
535 small RNA loci exists among a variety of Supergroup-A *Wolbachia* strains, suggesting
536 conservation within certain *Wolbachia* lineages (74). In the current study, a subset of the small
537 RNA-Seq reads within our libraries were found to originate from *w*AlbB, and two loci with
538 high coverage were predicted to form stem-loop structures, similar to those of canonical
539 miRNAs. It is possible that stem-loop structures within *w*AlbB non-coding RNAs could be
540 targeted by the host RNAi pathway. Although preliminary, these findings offer an intriguing
541 line of inquiry for future research.
542 A limitation of this study was the use of whole mosquitoes, rather than individual tissues.
543 Consequently, tissue-specific miRNAs would be underrepresented in the data, as more widely-
544 expressed miRNAs will have greatly outnumbered them at the whole-insect level. With some
545 miRNAs having very low normalised read counts, it is plausible that investigating certain
546 tissues rather than whole insects may allow investigation of some potentially informative
547 miRNAs that were underrepresented in our data.
548 Overall, our results show that *w*AlbB infection alters the miRNA expression profile of *Ae.*
549 *aegypti*. Some of the differentially expressed miRNAs reported here have been functionally
550 described in *Drosophila* or mosquitoes as having roles in innate immunity, ageing,
551 reproduction, development, or have been shown to be modulated by pathogens including
552 CHIKV and *w*MelPop. Further, we identified two miRNAs, miR-2946-3p, and miR-317-3p as
553 being potentially involved in symbiosis with *Wolbachia* via their effect on longevity in *w*AlbB-
554 infected mosquitoes. The results presented here serve to improve our understanding of the

555 molecular interactions governing the relationship between *Wolbachia* and its transinfected
556 host. Future research in this area should be directed at identifying the gene targets of *w*AlbB-
557 modulated miRNAs, followed by experimental manipulation of miRNAs and target genes to
558 determine the effect on *w*AlbB maintenance and host physiology.

559 **Acknowledgements**

560 Sassan Asgari is supported by the Australian Research Council (DP190102048). Cameron
561 Bishop is supported by a University of Queensland Research Higher Degree scholarship.

562 **Declaration of Interests**

563 The authors declare no conflicts of interests.

564 **Table 1: Differential expression of 46 miRNAs in WB2 vs WB2.tet mosquitoes in three**
565 **age groups**. Log_2 fold-changes > 0 represent upregulation in WB2 compared to WB2.tet. log_2
566 CPM, counts per million reads mapped to each miRNA given (log_2). FDR, false discovery rate
567 (Benjamini-Hochberg corrected p-value).

miRNA	log_2 CPM	log_2 FC	FDR	Age group
309a-3p	4.14	1.57	2.88E-04	2dpe
998-5p	5.05	1.30	2.12E-04	2dpe
10365-3p	4.77	0.76	1.44E-02	2dpe
2941-2-3p	11.74	0.72	4.98E-04	2dpe
11-5p	8.94	0.71	7.75E-03	2dpe
2765-5p	5.25	0.68	2.68E-02	2dpe
278-3p	12.10	0.65	1.44E-02	2dpe
2941-1-3p	8.94	0.59	8.11E-03	2dpe
965-5p	5.42	0.59	4.03E-02	2dpe
989-5p	5.39	0.57	2.10E-02	2dpe
1174-5p	5.86	0.56	3.60E-02	2dpe
100-3p	8.14	-0.50	1.23E-02	2dpe
1000-5p	7.54	-0.52	7.75E-03	2dpe
279-3p	12.73	-0.54	2.68E-02	2dpe
10365-5p	8.89	-0.55	1.44E-02	2dpe
12-5p	9.64	-0.58	2.10E-02	2dpe
let-7-5p	13.45	-0.67	2.10E-02	2dpe
31-3p	6.41	-0.73	7.75E-03	2dpe
276b-5p	6.37	-0.81	7.06E-04	2dpe
193-3p	2.40	-1.11	2.17E-02	2dpe
998-5p	5.05	0.94	9.98E-03	6dpe
308-5p	9.39	0.78	5.72E-06	6dpe
184-3p	14.72	0.70	9.95E-05	6dpe
13-5p	6.83	0.61	2.69E-02	6dpe
932-3p	6.60	0.59	1.84E-02	6dpe
100-5p	15.53	0.54	1.84E-02	6dpe
10-5p	13.41	0.53	1.23E-02	6dpe
12-5p	9.64	-0.52	3.39E-02	6dpe
13-3p	11.15	-0.54	2.69E-02	6dpe
277-3p	14.77	-0.54	9.98E-03	6dpe
9a-3p	5.22	-0.55	3.07E-02	6dpe
92a-3p	8.18	-0.56	9.98E-03	6dpe
965-3p	5.26	-0.57	3.77E-02	6dpe
1175-3p	10.50	-0.62	8.62E-03	6dpe
2940-5p	13.38	-0.64	1.23E-02	6dpe
996-3p	6.86	-0.66	3.73E-02	6dpe
190-5p	11.75	-0.80	2.45E-02	6dpe
2946-3p	9.98	-0.83	9.98E-03	6dpe
286b-3p	5.33	-0.84	1.23E-02	6dpe
219-5p	3.13	-0.92	3.03E-02	6dpe

980-5p	4.52	-0.96	3.03E-02	6dpe
2944a-5p	2.84	-1.17	2.45E-02	6dpe
2944b-3p	2.38	-1.60	1.84E-02	6dpe
2942-3p	3.84	-2.05	1.48E-06	6dpe
309a-3p	4.14	-0.69	3.79E-02	12dpe
2941-1-5p	3.39	-1.29	1.01E-02	12dpe
196-3p	2.93	-1.40	3.79E-02	12dpe

568

569 **Table 2: Differential expression of 31 miRNAs in older versus younger age groups in each**
570 **mosquito line**. Fold-changes > 0 represent upregulation in the older age group. $\log_2$ CPM,
571 counts per million reads mapped to each miRNA ($\log_2$).

			WB2.tet		WB2	
miRNA	**Contrast**	**$\log_2$ CPM**	**$\log_2$ FC**	**FDR**	**$\log_2$ FC**	**FDR**
1-5p	6dpe/2dpe	4.53	-1.15	1.6E-05	-	-
34-5p	6dpe/2dpe	15.31	-	-	1.20	4.3E-12
193-3p	6dpe/2dpe	2.40	-	-	-1.46	3.4E-04
193-5p	6dpe/2dpe	5.30	-1.11	2.6E-06	-1.58	3.1E-13
275-3p	6dpe/2dpe	13.00	-	-	-1.02	2.2E-10
286b-3p	6dpe/2dpe	5.33	-	-	1.16	4.1E-05
309a-3p	6dpe/2dpe	4.14	-	-	2.78	2.0E-21
317-3p	6dpe/2dpe	14.23	-	-	1.17	6.3E-15
2765-5p	6dpe/2dpe	5.25	-1.19	2.3E-05	-1.10	8.2E-05
2941-1-5p	6dpe/2dpe	3.39	-1.12	2.7E-03	-	-
2941-1-3p	6dpe/2dpe	8.94	-	-	1.13	5.9E-10
2941-2-3p	6dpe/2dpe	11.74	-	-	1.11	2.1E-10
2942-3p	6dpe/2dpe	3.84	-1.10	2.7E-02	-	-
2945-5p	6dpe/2dpe	3.51	-	-	-1.01	4.2E-04
2946-3p	6dpe/2dpe	9.98	-	-	1.12	3.3E-05
989-5p	6dpe/2dpe	5.39	-1.04	5.5E-06	-	-
1-5p	12dpe/2dpe	4.53	-1.13	3.6E-06	-1.34	2.6E-08
11893-5p	12dpe/2dpe	2.74	-	-	-1.03	1.9E-02
11894a-1-3p	12dpe/2dpe	3.68	1.21	3.5E-04	-	-
11894a-4-3p	12dpe/2dpe	5.02	1.56	1.3E-06	1.04	8.5E-04
11894b-3p	12dpe/2dpe	9.47	1.37	4.1E-08	1.10	9.5E-06
11899-5p	12dpe/2dpe	3.16	-1.42	3.7E-03	-2.43	3.0E-06
11899-3p	12dpe/2dpe	3.22	-	-	-1.97	4.1E-07
1890-5p	12dpe/2dpe	3.03	-	-	-1.51	1.6E-04
1890-3p	12dpe/2dpe	9.02	-1.15	1.1E-13	-1.02	2.8E-11
193-5p	12dpe/2dpe	5.30	-2.61	5.4E-28	-2.53	4.4E-28
193-3p	12dpe/2dpe	2.40	-	-	-1.38	7.8E-04
196-3p	12dpe/2dpe	2.93	-1.32	6.6E-03	-	-
275-3p	12dpe/2dpe	13.00	-1.04	6.6E-11	-	-

2765-5p	12dpe/2dpe	5.25	-2.03	5.3E-14	-1.86	2.1E-11
276b-5p	12dpe/2dpe	6.37	1.12	4.4E-08	-	-
277-3p	12dpe/2dpe	14.77	-	-	-1.01	1.1E-09
279-3p	12dpe/2dpe	12.73	1.04	3.3E-07	-	-
286b-3p	12dpe/2dpe	5.33	-	-	1.17	1.8E-05
2940-5p	12dpe/2dpe	12.40	1.45	1.1E-14	1.33	7.9E-13
2941-1-5p	12dpe/2dpe	3.39	-1.75	3.9E-07	-	-
2941-1-3p	12dpe/2dpe	8.94	-	-	1.23	8.7E-12
2941-2-3p	12dpe/2dpe	11.74	-	-	1.31	3.4E-14
2942-3p	12dpe/2dpe	3.84	-	-	-1.02	7.5E-03
2945-5p	12dpe/2dpe	3.51	-	-	-1.11	1.2E-04
2946-3p	12dpe/2dpe	9.98	1.29	7.0E-07	1.56	1.1E-09
309a-3p	12dpe/2dpe	4.14	1.21	1.1E-05	3.47	2.1E-37
317-3p	12dpe/2dpe	14.23	1.44	1.2E-22	1.67	5.2E-30
34-5p	12dpe/2dpe	15.31	1.19	4.5E-12	1.71	4.0E-24
92b-5p	12dpe/2dpe	4.43	-1.18	3.8E-04	-	-
980-3p	12dpe/2dpe	3.21	-	-	-1.22	5.8E-04
989-5p	12dpe/2dpe	5.39	-1.10	3.5E-07	-	-
996-3p	12dpe/2dpe	6.86	1.29	2.4E-06	-	-
999-5p	12dpe/2dpe	3.03	-1.13	6.3E-03	-	-
bantam-5p	12dpe/2dpe	10.55	-1.06	3.9E-07	-	-
196-3p	12dpe/6dpe	2.93	-1.42	1.5E-02	-	-
193-5p	12dpe/6dpe	5.30	-1.50	7.7E-08	-	-
11899-3p	12dpe/6dpe	3.22	-	-	-1.22	1.4E-02
11899-5p	12dpe/6dpe	3.16	-	-	-2.70	2.0E-06
1890-5p	12dpe/6dpe	3.03	-	-	-1.11	2.6E-02
980-3p	12dpe/6dpe	3.21	-	-	-1.32	4.7E-04
2942-3p	12dpe/6dpe	3.84	-	-	-1.41	3.8E-04
1-5p	6dpe/2dpe	4.53	-1.15	1.6E-05	-	-
34-5p	6dpe/2dpe	15.31	-	-	1.20	4.3E-12
193-3p	6dpe/2dpe	2.40	-	-	-1.46	3.4E-04
193-5p	6dpe/2dpe	5.30	-1.11	2.6E-06	-1.58	3.1E-13
275-3p	6dpe/2dpe	13.00	-	-	-1.02	2.2E-10
286b-3p	6dpe/2dpe	5.33	-	-	1.16	4.1E-05
309a-3p	6dpe/2dpe	4.14	-	-	2.78	2.0E-21
317-3p	6dpe/2dpe	14.23	-	-	1.17	6.3E-15
2765-5p	6dpe/2dpe	5.25	-1.19	2.3E-05	-1.10	8.2E-05
2941-1-5p	6dpe/2dpe	3.39	-1.12	2.7E-03	-	-
2941-1-3p	6dpe/2dpe	8.94	-	-	1.13	5.9E-10
2941-2-3p	6dpe/2dpe	11.74	-	-	1.11	2.1E-10
2942-3p	6dpe/2dpe	3.84	-1.10	2.7E-02	-	-
2945-5p	6dpe/2dpe	3.51	-	-	-1.01	4.2E-04
2946-3p	6dpe/2dpe	9.98	-	-	1.12	3.3E-05
989-5p	6dpe/2dpe	5.39	-1.04	5.5E-06	-	-
1-5p	12dpe/2dpe	4.53	-1.13	3.6E-06	-1.34	2.6E-08
11893-5p	12dpe/2dpe	2.74	-	-	-1.03	1.9E-02
11894a-1-3p	12dpe/2dpe	3.68	1.21	3.5E-04	-	-
11894a-4-3p	12dpe/2dpe	5.02	1.56	1.3E-06	1.04	8.5E-04
11894b-3p	12dpe/2dpe	9.47	1.37	4.1E-08	1.10	9.5E-06

11899-5p	12dpe/2dpe	3.16	-1.42	3.7E-03	-2.43	3.0E-06
11899-3p	12dpe/2dpe	3.22	-	-	-1.97	4.1E-07
1890-5p	12dpe/2dpe	3.03	-	-	-1.51	1.6E-04
1890-3p	12dpe/2dpe	9.02	-1.15	1.1E-13	-1.02	2.8E-11
193-5p	12dpe/2dpe	5.30	-2.61	5.4E-28	-2.53	4.4E-28
193-3p	12dpe/2dpe	2.40	-	-	-1.38	7.8E-04
196-3p	12dpe/2dpe	2.93	-1.32	6.6E-03	-	-
275-3p	12dpe/2dpe	13.00	-1.04	6.6E-11	-	-
2765-5p	12dpe/2dpe	5.25	-2.03	5.3E-14	-1.86	2.1E-11
276b-5p	12dpe/2dpe	6.37	1.12	4.4E-08	-	-
277-3p	12dpe/2dpe	14.77	-	-	-1.01	1.1E-09
279-3p	12dpe/2dpe	12.73	1.04	3.3E-07	-	-
286b-3p	12dpe/2dpe	5.33	-	-	1.17	1.8E-05

572

573 **Table 3: High confidence predicted targets of aae-miR-317-3p, and aae-miR-2946-3p.**

574 These predicted targets were subjected to RT-qPCR to determine if their expression could be

575 affected by age (Fig. S4).

miRNA	VectorBase accession no.	No. of predicted binding sites	Predicted target gene
317-3p	AAEL010793	7	F-box/leucine rich repeat protein
317-3p	AAEL006171	11	n-myc downstream regulated
317-3p	AAEL010508	11	vacuolar protein sorting-associated protein (vps13)
2946-3p	AAEL006095	5	Gelsolin precursor
2946-3p	AAEL006113	7	cystinosin
2946-3p	AAEL003402	9	sphingomyelin phosphodiesterase

576

577 **References**

578 1. Calvez E, Guillaumot L, Millet L, Marie J, Bossin H, Rama V, Faamoe A, Kilama S,
579 Teurlai M, Mathieu-Daudé F, Dupont-Rouzeyrol M. 2016. Genetic diversity and
580 phylogeny of *Aedes aegypti*, the main arbovirus vector in the Pacific. PLoS Neglected
581 Tropical Diseases 10:e0004374.
582 2. Lourenço-de-Oliveira R, Failloux A-B. 2017. High risk for chikungunya virus to
583 initiate an enzootic sylvatic cycle in the tropical Americas. PLoS Neglected Tropical
584 Diseases 11:e0005698.
585 3. Powell JR. 2018. Mosquito-borne human viral diseases: Why *Aedes aegypti*? American
586 Journal of Tropical Medicine and Hygiene 98:1563-1565.
587 4. Powell JR, Tabachnick WJ. 2013. History of domestication and spread of *Aedes*
588 *aegypti*--a review. Memórias do Instituto Oswaldo Cruz 108:11-17.
589 5. McGraw Ea, O'Neill SL. 2013. Beyond insecticides: new thinking on an ancient
590 problem. Nature Reviews Microbiology 11:181-193.
591 6. Scott J, Hardstone Yoshimizu M, Kasai S. 2015. Pyrethroid resistance in *Culex pipiens*
592 mosquitoes. Pesticide Biochemistry and Physiology 120:68-76.
593 7. Darrington M, Dalmay T, Morrison NI, Chapman T. 2017. Implementing the sterile
594 insect technique with RNA interference - a review. Entomologia Experimentalis et
595 Applicata 164:155-175.
596 8. Frentiu FD, Zakir T, Walker T, Popovici J, Pyke AT, van den Hurk A, McGraw EA,
597 O'Neill SL. 2014. Limited Dengue Virus Replication in Field-Collected *Aedes aegypti*
598 Mosquitoes Infected with *Wolbachia*. PLoS Neglected Tropical Diseases 8:e0002688.
599 9. Ranson H, Burhani J, Lumjuan N, Black IV WC. 2010. Insecticide resistance in dengue
600 vectors. TropIKAnet. 1: 1.
601 10. Frentiu FD, Robinson J, Young PR, McGraw EA, O'Neill SL. 2010. *Wolbachia*-
602 mediated resistance to dengue virus infection and death at the cellular level. PLoS ONE
603 5:e0013398.
604 11. Bourtzis K, Dobson SL, Xi Z, Rasgon JL, Calvitti M, Moreira LA, Bossin HC, Moretti
605 R, Baton LA, Hughes GL, Mavingui P, Gilles JRL. 2014. Harnessing mosquito-
606 *Wolbachia* symbiosis for vector and disease control. Acta Tropica 132:150-163.
607 12. Dobson SL. 2003. Reversing *Wolbachia*-based population replacement. Trends in
608 Parasitology 19:128-133.
609 13. Walker T, Johnson PH, Moreira La, Iturbe-Ormaetxe I, Frentiu FD, McMeniman CJ,
610 Leong YS, Dong Y, Axford J, Kriesner P, Lloyd aL, Ritchie Sa, O'Neill SL, Hoffmann
611 aa. 2011. The *w*Mel *Wolbachia* strain blocks dengue and invades caged *Aedes aegypti*
612 populations. Nature 476:450-453.
613 14. Nguyen TH, Nguyen HL, Nguyen TY, Vu SN, Tran ND, Le TN, Vien QM, Bui TC,
614 Le HT, Kutcher S, Hurst TP, Duong TTH, Jeffery JAL, Darbro JM, Kay BH, Iturbe-
615 Ormaetxe I, Popovici J, Montgomery BL, Turley AP, Zigterman F, Cook H, Cook PE,
616 Johnson PH, Ryan PA, Paton CJ, Ritchie SA, Simmons CP, O'Neill SL, Hoffmann AA.
617 2015. Field evaluation of the establishment potential of *w*MelPop *Wolbachia* in
618 Australia and Vietnam for dengue control. Parasites and Vectors 8:563.
619 15. Axford JK, Ross PA, Yeap HL, Callahan AG, Hoffmann AA. 2016. Fitness of *w*AlbB
620 *Wolbachia* Infection in *Aedes aegypti:* Parameter estimates in an outcrossed
621 background and potential for population invasion. American Journal of Tropical
622 Medicine and Hygiene 94:507-516.
623 16. Hoffmann A, Montgomery B, Popovici J, Iturbe-Ormaetxe I, Johnson P, Muzzi F,
624 Greenfield M, Durkan M, Leong Y, Dong Y, Cook H, Axford J, Callahan A, Kenny N,
625 Omodei C, McGraw E, Ryan P, Ritchie S, Turelli M, O'Neill S. 2011. Successful

626 establishment of *Wolbachia* in *Aedes* populations to suppress dengue transmission.
627 Nature 476:454-457.
628 17. Hoffmann AA, Ross PA, Rašić G. 2015. *Wolbachia* strains for disease control:
629 Ecological and evolutionary considerations. Evolutionary Applications 8:751-768.
630 18. Johnson KN. 2015. The impact of *Wolbachia* on virus infection in mosquitoes. Viruses
631 7:5705-5717.
632 19. Terradas G, Joubert DA, McGraw EA. 2017. The RNAi pathway plays a small part in
633 *Wolbachia*-mediated blocking of dengue virus in mosquito cells. Scientific Reports
634 7:43847.
635 20. Hussain M, Lu G, Torres S, Edmonds JH, Kay BH, Khromykh AA, Asgari S. 2013.
636 Effect of *Wolbachia* on replication of West Nile virus in a mosquito cell line and adult
637 mosquitoes. Journal of Virology 87:851-858.
638 21. Moreira LA, Iturbe-Ormaetxe I, Jeffery JA, Lu G, Pyke AT, Hedges LM, Rocha BC,
639 Hall-Mendelin S, Day A, Riegler M, Hugo LE, Johnson KN, Kay BH, McGraw EA,
640 van den Hurk AF, Ryan PA, O'Neill SL. 2009. A *Wolbachia* Symbiont in *Aedes aegypti*
641 Limits Infection with Dengue, Chikungunya, and Plasmodium. Cell 139:1268-1278.
642 22. McMeniman CJ, Lane RV, Cass BN, Fong AWC, Sidhu M, Wang YF, O'Neill SL.
643 2009. Stable introduction of a life-shortening *Wolbachia* infection into the mosquito
644 *Aedes aegypti*. Science 323:141-144.
645 23. Blagrove MSC, Arias-Goeta C, Failloux A-B, Sinkins SP. 2012. *Wolbachia* strain
646 *w*Mel induces cytoplasmic incompatibility and blocks dengue transmission in *Aedes*
647 *albopictus*. Proceedings of the National Academy of Sciences, USA 109:255-260.
648 24. Hoffmann AA, Iturbe-Ormaetxe I, Callahan AG, Phillips BL, Billington K, Axford JK,
649 Montgomery B, Turley AP, O'Neill SL. 2014. Stability of the *w*Mel *Wolbachia*
650 Infection following Invasion into *Aedes aegypti* Populations. PLoS Neglected Tropical
651 Diseases 8:e0003115.
652 25. Ross PA, Wiwatanaratanabutr I, Axford JK, White VL, Endersby-Harshman NM,
653 Hoffmann AA. 2017. *Wolbachia* infections in *Aedes aegypti* differ markedly in their
654 response to cyclical heat stress. PLoS Pathogens 13:e1006006.
655 26. Ulrich JN, Beier JC, Devine GJ, Hugo LE. 2016. Heat sensitivity of *w*Mel *Wolbachia*
656 during *Aedes aegypti* development. PLoS Neglected Tropical Diseases 10:e0004873.
657 27. Acosta EG, Castilla V, Damonte EB. 2008. Functional entry of dengue virus into *Aedes*
658 *albopictus* mosquito cells is dependent on clathrin-mediated endocytosis. Journal of
659 General Virology 89:474-484.
660 28. Bian G, Xu Y, Lu P, Xie Y, Xi Z. 2010. The endosymbiotic bacterium *Wolbachia*
661 induces resistance to dengue virus in *Aedes aegypti*. PLoS Pathogens 6:e1000833.
662 29. Nazni WA, Hoffmann AA, NoorAfizah A, Cheong YL, Mancini MV, Golding N,
663 Kamarul GMR, Arif MAK, Thohir H, NurSyamimi H, ZatilAqmar MZ, NurRuqqayah
664 M, NorSyazwani A, Faiz A, Irfan FRMN, Rubaaini S, Nuradila N, Nizam NMN, Irwan
665 SM, Endersby-Harshman NM, White VL, Ant TH, Herd CS, Hasnor AH, AbuBakar R,
666 Hapsah DM, Khadijah K, Kamilan D, Lee SC, Paid YM, Fadzilah K, Topek O, Gill
667 BS, Lee HL, Sinkins SP. 2019. Establishment of *Wolbachia* Strain *w*AlbB in Malaysian
668 Populations of *Aedes aegypti* for Dengue Control. Current Biology 29:4241-4248.
669 30. Xi Z, Khoo CCH, Dobson SL. 2005. *Wolbachia* establishment and invasion in an Aedes
670 aegypti laboratory population. Science 310:326-8.
671 31. Kremer N, Charif D, Henri H, Gavory F, Wincker P, Mavingui P, Vavre F. 2012.
672 Influence of *Wolbachia* on host gene expression in an obligatory symbiosis. BMC
673 Microbiology 12:S7.
674 32. Pan X, Zhou G, Wu J, Bian G, Lu P, Raikhel AS, Xi Z. 2012. *Wolbachia* induces
675 reactive oxygen species (ROS)-dependent activation of the Toll pathway to control

676 dengue virus in the mosquito *Aedes aegypti*. Proceedings of the National Academy of
677 Sciences, USA 109:E23-E31.
678 33. Pan X, Pike A, Joshi D, Bian G, McFadden MJ, Lu P, Liang X, Zhang F, Raikhel AS,
679 Xi Z. 2018. The bacterium Wolbachia exploits host innate immunity to establish a
680 symbiotic relationship with the dengue vector mosquito *Aedes aegypti*. ISME J 12:277-
681 288.
682 34. Xi Z, Gavotte L, Xie Y, Dobson SL. 2008. Genome-wide analysis of the interaction
683 between the endosymbiotic bacterium *Wolbachia* and its *Drosophila* host. BMC
684 Genomics 9:1.
685 35. Brennan LJ, Haukedal JA, Earle JC, Keddie B, Harris HL. 2012. Disruption of redox
686 homeostasis leads to oxidative DNA damage in spermatocytes of *Wolbachia*-infected
687 *Drosophila* simulans. Insect Molecular Biology 21:510-520.
688 36. Grobler Y, Yun CY, Kahler DJ, Bergman CM, Lee H, Oliver B, Lehmann R. 2018.
689 Whole genome screen reveals a novel relationship between *Wolbachia* and *Drosophila*
690 host translation. PLoS Pathogens 14:e1007445.
691 37. White PM, Serbus LR, Debec A, Codina A, Bray W, Guichet A, Lokey RS, Sullivan
692 W, Pamela M. White LRS, Alain Debec, Adan Codina, Walter Bray, Antoine Guichet,
693 R. Scott Lokey, William Sullivan. 2017. Reliance of *Wolbachia* on High Rates of Host
694 Proteolysis Revealed by a Genome-Wide RNAi Screen of *Drosophila* Cells. Genetics
695 205:1473-1488.
696 38. Newton ILG, Rice DW. 2020. The Jekyll and Hyde symbiont: Could *Wolbachia* be a
697 nutritional mutualist? Journal of Bacteriology 202:e00589-19.
698 39. Kremer N, Voronin D, Charif D, Mavingui P, Mollereau B, Vavre F. 2009. *Wolbachia*
699 interferes with ferritin expression and iron metabolism in insects. PLoS Pathogens
700 5:e1000630.
701 40. Bartel DP. 2009. MicroRNAs: Target recognition and regulatory functions. Cell
702 136:215-233.
703 41. Feng X, Zhou S, Wang J, Hu W. 2018. microRNA profiles and functions in mosquitoes.
704 PLoS Neglected Tropical Diseases 12:e0006463.
705 42. Nouzova M, Etebari K, Noriega FG, Asgari S. 2018. A comparative analysis of corpora
706 allata-corpora cardiaca microRNA repertoires revealed significant changes during
707 mosquito metamorphosis. Insect Biochemistry and Molecular Biology 96:10-18.
708 43. Zhang Y, Zhao B, Roy S, Saha TT, Kokoza VA, Li M, Raikhel AS. 2016. microRNA-
709 309 targets the Homeobox gene *SIX4* and controls ovarian development in the mosquito
710 *Aedes aegypti*. Proceedings of the National Academy of Sciences, USA 113:E4828-
711 E4836.
712 44. Liu S, Lucas KJ, Roy S, Ha J, Raikhel AS. 2014. Mosquito-specific microRNA-1174
713 targets serine hydroxymethyltransferase to control key functions in the gut. Proceedings
714 of the National Academy of Sciences, USA 111:14460-14465.
715 45. Yen PS, Chen CH, Sreenu V, Kohl A, Failloux AB. 2019. Assessing the potential
716 interactions between cellular miRNA and arboviral genomic RNA in the yellow fever
717 mosquito, *Aedes aegypti*. Viruses 11:540.
718 46. Dubey SK, Shrinet J, Sunil S. 2019. *Aedes aegypti* microRNA, miR-2944b-5p interacts
719 with 3'UTR of chikungunya virus and cellular target vps-13 to regulate viral
720 replication. PLoS Neglected Tropical Diseases 13:e0007429.
721 47. Hussain M, Walker T, O'Neill SL, Asgari S. 2013. Blood meal induced microRNA
722 regulates development and immune associated genes in the Dengue mosquito vector,
723 *Aedes aegypti*. Insect Biochemistry and Molecular Biology 43:146-152.
724 48. Zhang G, Hussain M, O'Neill SL, Asgari S. 2013. *Wolbachia* uses a host microRNA to
725 regulate transcripts of a methyltransferase, contributing to dengue virus inhibition in

Aedes aegypti. Proceedings of the National Academy of Sciences, USA 110:10276-10281.

49. Zhang G, Hussain M, Asgari S. 2014. Regulation of arginine methyltransferase 3 by a *Wolbachia*-induced microRNA in *Aedes aegypti* and its effect on *Wolbachia* and dengue virus replication. Insect Biochemistry and Molecular Biology 53:81-88.
50. Slonchak A, Hussain M, Torres S, Asgari S, Khromykh AA. 2014. Expression of mosquito microRNA aae-miR-2940-5p is downregulated in response to West Nile virus infection to restrict viral replication. Journal of Virology 88:8457-8467.
51. Beebe NW, Pagendam D, Trewin BJ, Boomer A, Bradford M, Ford A, Liddington C, Bondarenco A, De Barro PJ, Gilchrist JJPotNAoS. 2021. Releasing incompatible males drives strong suppression across populations of wild and *Wolbachia*-carrying *Aedes aegypti* in Australia. Proceedings of the National Academy of Sciences, USA 118: e2106828118.
52. Parry R, Bishop C, De Hayr L, Asgari S. 2019. Density-dependent enhanced replication of a densovirus in *Wolbachia*-infected *Aedes* cells is associated with production of piRNAs and higher virus-derived siRNAs. Virology 528:89-100.
53. Bushnell B. Sponsor Org.: USDOE Office of Science (SC). BBMap: A Fast, Accurate, Splice-Aware Aligner, p. *In* (ed), Research Org.: Lawrence Berkeley National Lab. (LBNL), Berkeley, CA (United States).
54. Andrews S. 2010. FastQC: a quality control tool for high throughput sequence data.
55. Friedländer MR, MacKowiak SD, Li N, Chen W, Rajewsky N. 2012. MiRDeep2 accurately identifies known and hundreds of novel microRNA genes in seven animal clades. Nucleic Acids Research 40:37-52.
56. Kozomara A, Birgaoanu M, Griffiths-Jones S. 2018. miRBase: from microRNA sequences to function. Nucleic Acids Research 47:155-162.
57. Zhang Z, Schwartz S, Wagner L, Miller W. 2000. A greedy algorithm for aligning DNA sequences. Journal of Computational Biology 7:203-214.
58. Matthews BJ, Dudchenko O, Kingan SB, Koren S, Antoshechkin I, Crawford JE, Glassford WJ, Herre M, Redmond SN, Rose NH, Weedall GD, Wu Y, Batra SS, Brito-Sierra CA, Buckingham SD, Campbell CL, Chan S, Cox E, Evans BR, Fansiri T, Filipović I, Fontaine A, Gloria-Soria A, Hall R, Joardar VS, Jones AK, Kay RGG, Kodali VK, Lee J, Lycett GJ, Mitchell SN, Muehling J, Murphy MR, Omer AD, Partridge FA, Peluso P, Aiden AP, Ramasamy V, Rašić G, Roy S, Saavedra-Rodriguez K, Sharan S, Sharma A, Smith ML, Turner J, Weakley AM, Zhao Z, Akbari OS, Black WC, Cao H, et al. 2018. Improved reference genome of *Aedes aegypti* informs arbovirus vector control. Nature 563:501-507.
59. Johnson NR, Yeoh JM, Coruh C, Axtell MJ. 2016. Improved placement of multi-mapping small RNAs. G3: Genes, Genomes, Genetics 6:2103-2111.
60. Robinson MD, McCarthy DJ, Smyth GK. 2010. edgeR: a Bioconductor package for differential expression analysis of digital gene expression data. J Bioinformatics 26:139-140.
61. Robinson MD, Oshlack A. 2010. A scaling normalization method for differential expression analysis of RNA-seq data. J Bioinformatics 11:R25.
62. Wood DE, Lu J, Langmead B. 2019. Improved metagenomic analysis with Kraken 2. Genome Biology 20:257.
63. Ondov BD, Bergman NH, Phillippy AM. 2011. Interactive metagenomic visualization in a Web browser. BMC Bioinformatics 12:385.
64. John B, Enright AJ, Aravin A, Tuschl T, Sander C, Marks DS. 2004. Human microRNA targets. PLoS Biol 2:e363.

775 65. Miranda KC, Huynh T, Tay Y, Ang Y-S, Tam W-L, Thomson AM, Lim B, Rigoutsos
776 I. 2006. A pattern-based method for the identification of microRNA binding sites and
777 their corresponding heteroduplexes. Cell 126:1203-1217.
778 66. Kertesz M, Iovino N, Unnerstall U, Gaul U, Segal E. 2007. The role of site accessibility
779 in microRNA target recognition. Nature Genetics 39:1278-84.
780 67. Giraldo-Calderon GI, Emrich SJ, MacCallum RM, Maslen G, Dialynas E, Topalis P,
781 Ho N, Gesing S, Madey G, Collins FH, Lawson D. 2015. VectorBase: an updated
782 bioinformatics resource for invertebrate vectors and other organisms related with
783 human diseases. Nucleic Acids Research 43:D707-13.
784 68. Sinha A, Li Z, Sun L, Carlow CKS. 2019. Complete Genome Sequence of the
785 Wolbachia *w*AlbB Endosymbiont of *Aedes albopictus*. Genome Biology and Evolution
786 11:706-720.
787 69. Langmead B, Salzberg SL. 2012. Fast gapped-read alignment with Bowtie 2. Nature
788 Methods 9:357-359.
789 70. Quinlan AR. 2014. BEDTools: The Swiss-Army Tool for Genome Feature Analysis.
790 Current Protocols in Bioinformatics 47:11.12.1-11.12.34.
791 71. Lorenz R, Bernhart SH, Höner zu Siederdissen C, Tafer H, Flamm C, Stadler PF,
792 Hofacker IL. 2011. ViennaRNA Package 2.0. Algorithms for Molecular Biology 6:26.
793 72. Ridley A, Hereward J, Daglish G, Raghu S, McCulloch G, Walter G. 2016. Flight of
794 Rhyzopertha dominica (Coleoptera: Bostrichidae)—a spatio-temporal analysis with
795 pheromone trapping and population genetics. Journal of Economic Entomology
796 109:2561-2571.
797 73. Nene V, Wortman JR, Lawson D, Haas B, Kodira C, Tu ZJ, Loftus B, Xi Z, Megy K,
798 Grabherr M, Ren Q, Zdobnov EM, Lobo NF, Campbell KS, Brown SE, Bonaldo MF,
799 Zhu J, Sinkins SP, Hogenkamp DG, Amedeo P, Arensburger P, Atkinson PW, Bidwell
800 S, Biedler J, Birney E, Bruggner RV, Costas J, Coy MR, Crabtree J, Crawford M,
801 Debruyn B, Decaprio D, Eiglmeier K, Eisenstadt E, El-Dorry H, Gelbart WM, Gomes
802 SL, Hammond M, Hannick LI, Hogan JR, Holmes MH, Jaffe D, Johnston JS, Kennedy
803 RC, Koo H, Kravitz S, Kriventseva EV, Kulp D, Labutti K, Lee E, et al. 2007. Genome
804 sequence of *Aedes aegypti*, a major arbovirus vector. Science 316:1718-23.
805 74. Mayoral JG, Hussain M, Joubert DA, Iturbe-Ormaetxe I, O'Neill SL, Asgari S. 2014.
806 *Wolbachia* small noncoding RNAs and their role in cross-kingdom communications.
807 Proceedings of the National Academy of Sciences, USA 111:18721-18726.
808 75. Lee Y, Jeon K, Lee JT, Kim S, Kim VN. 2002. MicroRNA maturation: stepwise
809 processing and subcellular localization. The EMBO journal 21:4663-4670.
810 76. Gu J, Hu W, Wu J, Zheng P, Chen M, James AA, Chen X, Tu Z. 2013. miRNA genes
811 of an invasive vector mosquito, *Aedes albopictus*. PLoS ONE 8:e0067638.
812 77. Li S, Mead Ea, Liang S, Tu Z. 2009. Direct sequencing and expression analysis of a
813 large number of miRNAs in *Aedes aegypti* and a multi-species survey of novel
814 mosquito miRNAs. BMC Genomics 10:581.
815 78. Mayoral JG, Etebari K, Hussain M, Khromykh AA, Asgari S. 2014. *Wolbachia*
816 infection modifies the profile, shuttling and structure of microRNAs in a mosquito cell
817 line. PLoS ONE 9:e0096107.
818 79. Zhou L, Lim MYT, Kaur P, Saj A, Bortolamiol-Becet D, Gopal V, Tolwinski N,
819 Tucker-Kellogg G, Okamura K. 2018. Importance of miRNA stability and alternative
820 primary miRNA isoforms in gene regulation during *Drosophila* development. eLife
821 7:e38389.
822 80. Xiong X-P, Kurthkoti K, Chang K-Y, Li J-L, Ren X, Ni J-Q, Rana TM, Zhou R. 2016.
823 miR-34 modulates innate immunity and ecdysone signaling in *Drosophila*. PLoS
824 Pathogens 12:e1006034.

825 81. Liu N, Landreh M, Cao K, Abe M, Hendriks GJ, Kennerdell JR, Zhu Y, Wang LS,
826 Bonini NM. 2012. The microRNA miR-34 modulates ageing and neurodegeneration in
827 *Drosophila*. Nature 482:519-523.
828 82. Atilano ML, Glittenberg M, Monteiro A, Copley RR, Ligoxygakis P. 2017.
829 MicroRNAs that contribute to coordinating the immune response in *Drosophila*
830 *melanogaster*. Genetics 207:163-178.
831 83. Winter F, Edaye S, Hüttenhofer A, Brunel C. 2007. *Anopheles gambiae* miRNAs as
832 actors of defence reaction against *Plasmodium* invasion. Nucleic Acids Research
833 35:6953-6962.
834 84. Hussain M, Frentiu FD, Moreira LA, O'Neill SL, Asgari S. 2011. *Wolbachia* uses host
835 microRNAs to manipulate host gene expression and facilitate colonization of the
836 dengue vector *Aedes aegypti*. Proceedings of the National Academy of Sciences, USA
837 108:9250-9255.
838 85. Joanne S, Vythilingam I, Yugavathy N, Leong CS, Wong ML, AbuBakar S. 2015.
839 Distribution and dynamics of *Wolbachia* infection in Malaysian *Aedes albopictus*. Acta
840 Tropica 148:38-45.
841 86. Thomas S, Verma J, Woolfit M, O'Neill SL. 2018. Wolbachia-mediated virus blocking
842 in mosquito cells is dependent on XRN1-mediated viral RNA degradation and
843 influenced by viral replication rate. PLoS Pathogens 14:e1006879.
844 87. Rainey SM, Martinez J, McFarlane M, Juneja P, Sarkies P, Lulla A, Schnettler E,
845 Varjak M, Merits A, Miska EA, Jiggins FM, Kohl A. 2016. *Wolbachia* blocks viral
846 genome replication early in infection without a transcriptional response by the
847 endosymbiont or host small RNA pathways. PLoS Pathogens 12:e1005536.
848 88. Monsanto-Hearne V, Johnson KN. 2018. *Wolbachia*-mediated protection of
849 *Drosophila melanogaster* against systemic infection with its natural viral pathogen
850 Drosophila C virus does not involve changes in levels of highly abundant miRNAs.
851 Journal of General Virology 99:827-831.
852 89. Asad S, Hussain M, Hugo L, Osei-Amo S, Zhang G, Watterson D, Asgari S. 2018.
853 Suppression of the pelo protein by *Wolbachia* and its effect on dengue virus in *Aedes*
854 *aegypti*. PLoS Neglected Tropical Diseases 12:e0006405.

855 **Figure legends**

856 **Figure 1: *w*AlbB density in WB2 mosquitoes and results of read mapping. A)** Relative
857 *w*AlbB density at 2, 6, and 12 dpe. Crossbars represent the mean of three replicates (n=3).
858 Density of *w*AlbB was not significantly different between age groups (ANOVA, $p > 0.05$).
859 Error bars represent SEM. **B)** Number of forward- and reverse-mapped reads to the *Ae. aegypti*
860 AaegL5.0 genome after size selection and quality filtering. **C)** Reads that did not align to the
861 *Ae. aegypti* genome were aligned to the *Wolbachia w*AlbB genome. Each point represents the
862 proportion of non-*Ae. aegypti* reads that mapped to *Wolbachia w*AlbB.

863 **Figure 2: Position of miRNA loci on *Ae. aegypti* chromosomes.** Map of the three *Ae. aegypti*
864 chromosomes showing position, strand, and genomic context (i.e. intronic, exonic, or
865 intergenic) of precursor miRNA loci. Gene identifiers with 'LOC' prefix indicate parent genes
866 of intronic or exonic miRNA loci.

867 **Figure 3: Differentially expressed miRNAs in WB2 vs. WB2.tet mosquitoes. A)** Principal
868 components analysis of $\log_2$ normalised counts of 168 miRNAs showing separation of WB2
869 and WB2.tet mosquitoes in each of the three age groups with respect to miRNA expression.
870 Ellipses show 95% C.I. **B)** Volcano plots show differential expression of miRNAs in each age
871 group. Proportion of up- and down-regulated miRNAs is approximately equal at 2 dpe, but
872 becomes skewed toward downregulation in 6 dpe and 12 dpe. Red dots represent miRNAs that
873 meet the cut-off for FDR (q) and $\log_2$ fold-change; green, those that meet $\log_2$ fold-change cut-
874 off, but not q significant; blue, those that meet the q significance but not the $\log_2$ fold-change
875 cut-off; grey, those that meet neither cut-off. **C)** Venn diagram showing overlap in significantly
876 differentially expressed miRNAs between three age groups: 2 dpe, 6 dpe and 12 dpe. There
877 was limited overlap between age groups. Only two miRNAs, miR-12-5p and miR-998-5p were
878 in common between 2 dpe and 6 dpe. A third miRNA, miR-309a-3p, was down-regulated at 2
879 dpe and up-regulated at 12 dpe. **D)** Pairwise comparisons of $\log_2$ fold-changes of miRNAs that

880 were significant in one age group (x-axis) against the same miRNAs in another age group (y-
881 axis). All Pearson correlations were significant ($p < 0.05$).

882 **Figure 4: Validation of selected differentially expressed miRNAs.** Plots show $\log_2$ fold
883 changes of a selection of miRNAs according to small RNA-Seq and RT-qPCR at 2, 6, and 12
884 days post-emergence using 5S RNA for normalization of data. Bars are averages of three
885 biological replicates. Error bars show standard error of the mean.

886 **Figure 5: Expression of *Ae. aegypti* miRNAs increasing with age**. **A)** Venn diagram showing
887 overlap in significantly differentially expressed miRNAs between two mosquito lines. Age-
888 related differential expression of miRNAs showed a reasonable degree of overlap between
889 lines, with 14 out of 34 miRNAs (41%) being differentially expressed with age in both WB2
890 and WB2.tet mosquitoes. **B)** Graphs showing results of RT-qPCR of six miRNAs that showed
891 significant differential expression between age groups according to RNA-Seq. miRNAs in
892 WB2 mosquitoes were lower in abundance at 2 dpe compared to WB2.tet, but generally
893 increased with age more steeply. Points are averages of three biological replicates. Error bars
894 represent standard error of the mean. Significant difference between means was estimated
895 using a factorial ANOVA ($p < 0.05$). NS, not significant.

896 **Figure 6: Differential expression of selected potential targets of aae-miR-317-3p (top row)**
897 **and aae-miR-2946-3p (bottom row) that were differentially expressed with mosquito age.**
898 RT-qPCR analysis of RNA extracted from mosquitoes at 2, 6, and 12 dpe using primers to the
899 target genes and *rps17* as the normalizing gene. Two-way ANOVA with post-hoc multiple
900 comparisons was carried out to compare the expression levels between different time points.
901 Different letters on top of each time point represent statistically significant differences.

902 **Figure 7: *w*AlbB density in miRNA inhibited Aag2.*w*AlbB cells**. **A)** *w*AlbB density of
903 Aag2.*w*AlbB cells following transfection with specific miRNA inhibitors, random negative
904 control (NC) or Cellfectin only. **B and C)** Validation of inhibition of miR-190-5p, and miR-

905 276b-5p by RT-qPCR in the samples used in A. Cross-bars represent the mean of three
906 replicates. Asterisks indicate the level of statistical significance determined using to ANOVA.
907 *, $p < 0.05$; **, $p < 0.01$.

908 **Figure 8: inhibition of miR-317-3p and miR-2946-3p and its effect on lifespan of adult *Ae.***
909 ***aegypti* females**. **A and B)** Effect of miRNA inhibition on relative expression of miR-317-3p
910 in WB2.tet and WB2 mosquitoes, respectively. **C and D)** Effect of miRNA inhibition on
911 relative expression of miR-2946-3p in WB2.tet and WB2 mosquitoes respectively. **E and F)**
912 Effect of miRNA inhibition on longevity of WB2.tet and WB2 mosquitoes, respectively. KD,
913 knock down. WB2.tet survival was not significantly affected by miRNA inhibition. WB2
914 survival was significantly affected by inhibition of miR-2946-3p (Cox ph, $p < 0.0001$) and
915 miR-317-3p (Cox ph, $p = 0.013$).

916

917 **Supplementary Material legends**

918 **Figure S1:** Read-length distribution of small RNA-Seq libraries.

919 **Figure S2: Bacterial community composition is consistent between WB2 and WB2.tet**
920 **mosquitoes**. Results of Kraken analysis of reads that did not map to either **A)** *Ae. aegypti* or
921 *w*AlbB in WB2 mosquitoes, or **B)** *Ae. aegypti* in WB2.tet mosquitoes.

922 **Figure S3:** Per-base small RNA-SEQ read depth of the predicted hairpin corresponding to
923 Peak1.

924 **Figure S4:** Per-base small RNA-SEQ read depth of the predicted hairpin corresponding to
925 Peak 9.

926 **Figure S5: *w*AlbB-derived miRNA-like small RNAs. (A)** Predicted hairpin structures
927 corresponding to two regions of the *w*AlbB NZ_CP031221.1 genome that had high coverage
928 of small RNA-Seq reads in libraries derived from WB2 mosquitos. Genomic coordinates
929 indicate the start and end positions of the putative hairpin structure, identified by two peaks of

930 18-24nt long small RNA-Seq reads. **(B)** Sequence alignment between each predicted stem-loop
931 structure and *W*snRNA-46 and *W*snRNA-59 from Mayoral et al., 2014. Dots represent
932 homologous positions.
933 **Table S1.** Primers and oligos used in this study.
934 **Table S2:** Small RNA-Seq QC mapping statistics.
935 **Table S3:** Genomic coordinates of precursor and mature miRNA loci in the AaeL5.0 reference
936 genome. The base mean is the mean of counts of all samples, normalized for sequencing depth.
937 **Table S4.** Validation of small RNA-Seq using RT-qPCR for nine miRNAs using 5s ribosomal
938 RNA as reference. Ct, cycle threshold. FC, fold-change. CPM, counts per million.
939 **Table S5.** Peaks in coverage of small RNA-Seq reads aligned to the *w*AlbB NZ_CP031221.1.
940 'w2', 'w6', 'w12' refer to WB2 2 dpe, WB2 6 dpe, and WB2 12 dpe, respectively. Two
941 intergenic regions containing peaks 1 and 9 showed a pattern of read-coverage reminiscent of
942 precursor miRNA loci, and were predicted to form stem-loop structures (Figs. S3-5A).

Fig. 1

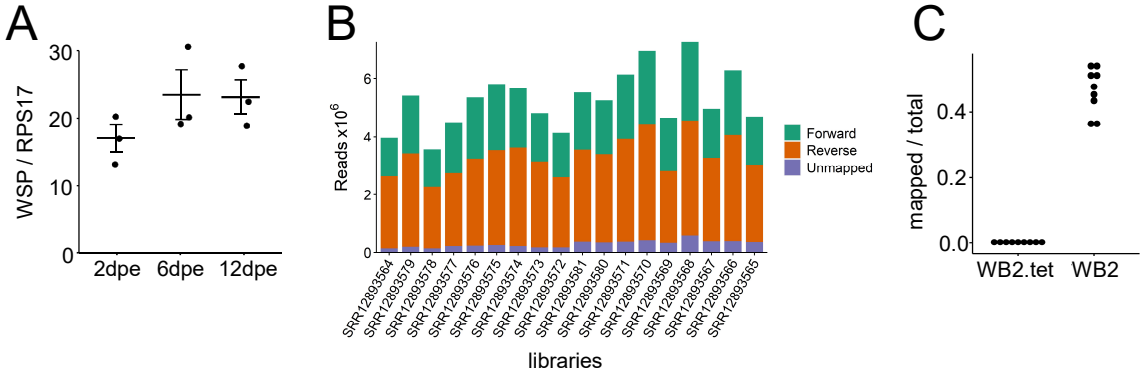
A
WSP / RPS17
30
20
10
0
2dpe
6dpe
12dpe
B
Reads x10^6
6
4
2
0
SRR12893564
SRR12893579
SRR12893578
SRR12893577
SRR12893576
SRR12893575
SRR12893574
SRR12893573
SRR12893572
SRR12893581
SRR12893580
SRR12893571
SRR12893570
SRR12893569
SRR12893568
SRR12893567
SRR12893566
SRR12893565
libraries
Forward
Reverse
Unmapped
C
mapped / total
0.4
0.2
0.0
WB2.tet
WB2

Fig. 2

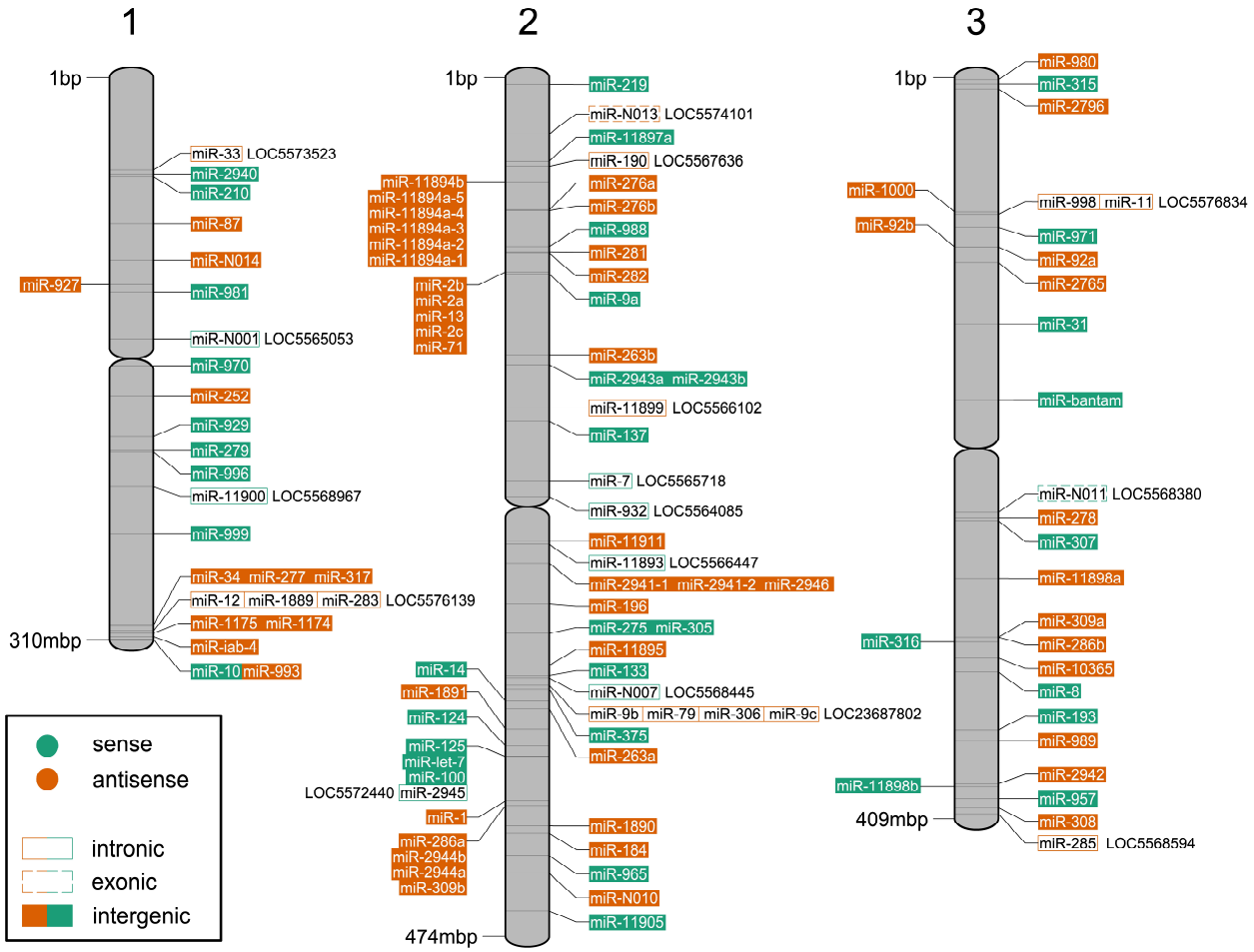
1
2
3
1bp
310mbp
miR-33 LOC5573523
miR-2940
miR-210
miR-87
miR-N014
miR-927
miR-981
miR-N001 LOC5565053
miR-970
miR-252
miR-929
miR-279
miR-996
miR-11900 LOC5568967
miR-999
miR-34 miR-277 miR-317
miR-12 miR-1889 miR-283 LOC5576139
miR-1175 miR-1174
miR-iab-4
miR-10 miR-993
sense
antisense
intronic
exonic
intergenic
1bp
474mbp
miR-219
miR-N013 LOC5574101
miR-11897a
miR-190 LOC5567636
miR-11894b
miR-11894a-5
miR-11894a-4
miR-11894a-3
miR-11894a-2
miR-11894a-1
miR-276a
miR-276b
miR-988
miR-281
miR-282
miR-2b
miR-2a
miR-13
miR-2c
miR-71
miR-9a
miR-263b
miR-2943a miR-2943b
miR-11899 LOC5566102
miR-137
miR-7 LOC5565718
miR-932 LOC5564085
miR-11911
miR-11893 LOC5566447
miR-2941-1 miR-2941-2 miR-2946
miR-196
miR-275 miR-305
miR-11895
miR-133
miR-N007 LOC5568445
miR-9b miR-79 miR-306 miR-9c LOC23687802
miR-375
miR-263a
miR-14
miR-1891
miR-124
miR-125
miR-let-7
miR-100
LOC5572440 miR-2945
miR-1
miR-286a
miR-2944b
miR-2944a
miR-309b
miR-1890
miR-184
miR-965
miR-N010
miR-11905
1bp
409mbp
miR-980
miR-315
miR-2796
miR-1000
miR-92b
miR-998 miR-11 LOC5576834
miR-971
miR-92a
miR-2765
miR-31
miR-bantam
miR-N011 LOC5568380
miR-278
miR-307
miR-11898a
miR-316
miR-309a
miR-286b
miR-10365
miR-8
miR-193
miR-989
miR-11898b
miR-2942
miR-957
miR-308
miR-285 LOC5568594

Fig. 3

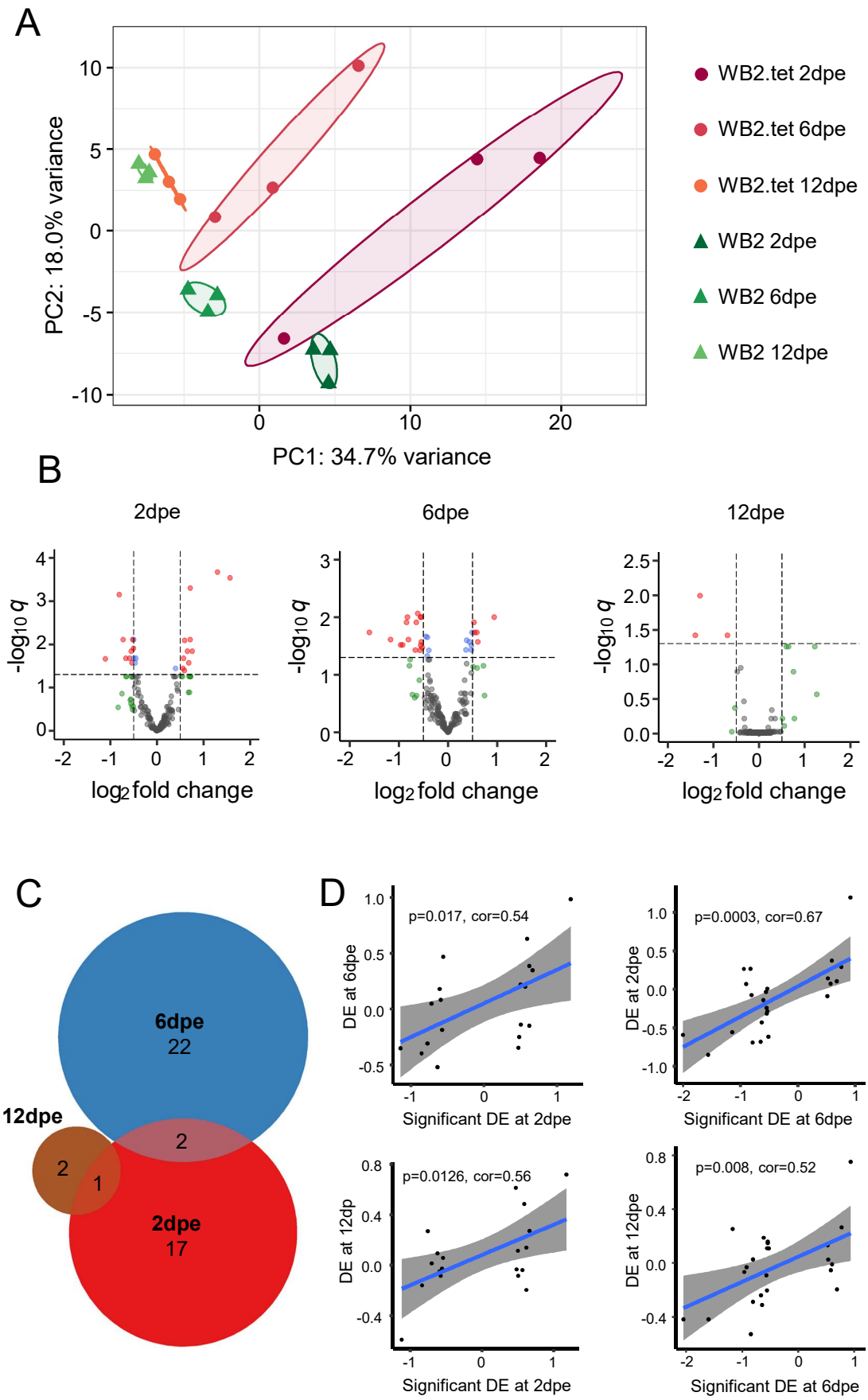
A
PC2: 18.0% variance
PC1: 34.7% variance
WB2.tet 2dpe
WB2.tet 6dpe
WB2.tet 12dpe
WB2 2dpe
WB2 6dpe
WB2 12dpe
B
2dpe
6dpe
12dpe
-log10 q
log2 fold change
C
6dpe
22
12dpe
2
2
1
2dpe
17
D
p=0.017, cor=0.54
DE at 6dpe
Significant DE at 2dpe
p=0.0003, cor=0.67
DE at 2dpe
Significant DE at 6dpe
p=0.0126, cor=0.56
DE at 12dp
Significant DE at 2dpe
p=0.008, cor=0.52
DE at 12dpe
Significant DE at 6dpe

Fig. 4

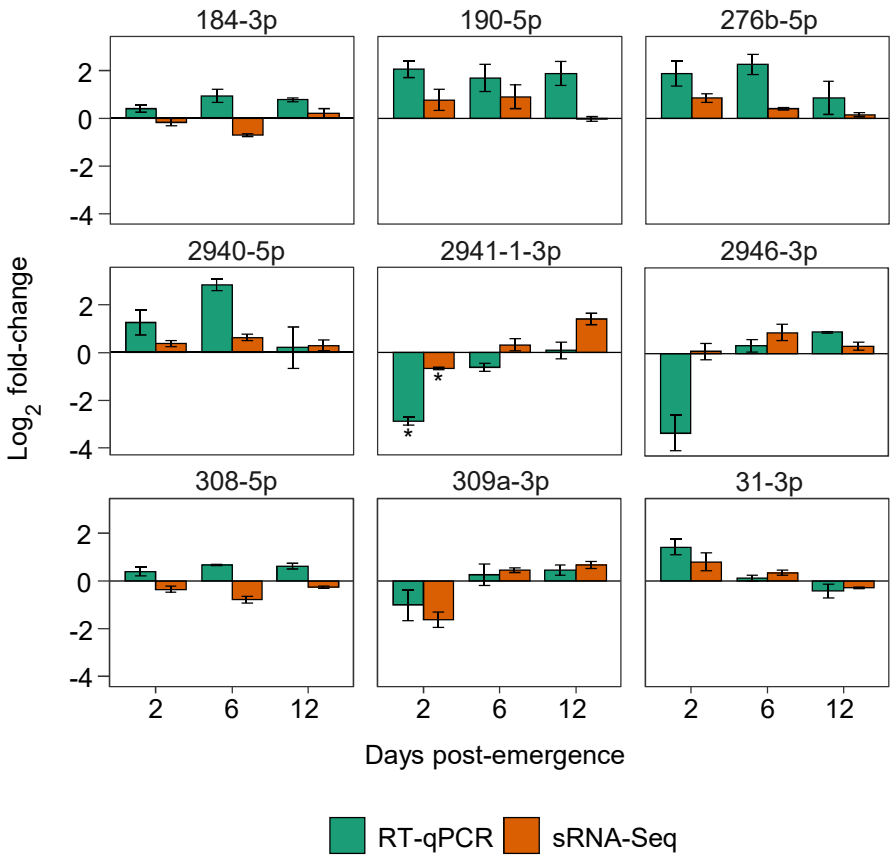
184-3p
190-5p
276b-5p
2940-5p
2941-1-3p
2946-3p
308-5p
309a-3p
31-3p
Log2 fold-change
2
0
-2
-4
*
2
6
12
Days post-emergence
RT-qPCR
sRNA-Seq

Fig. 5

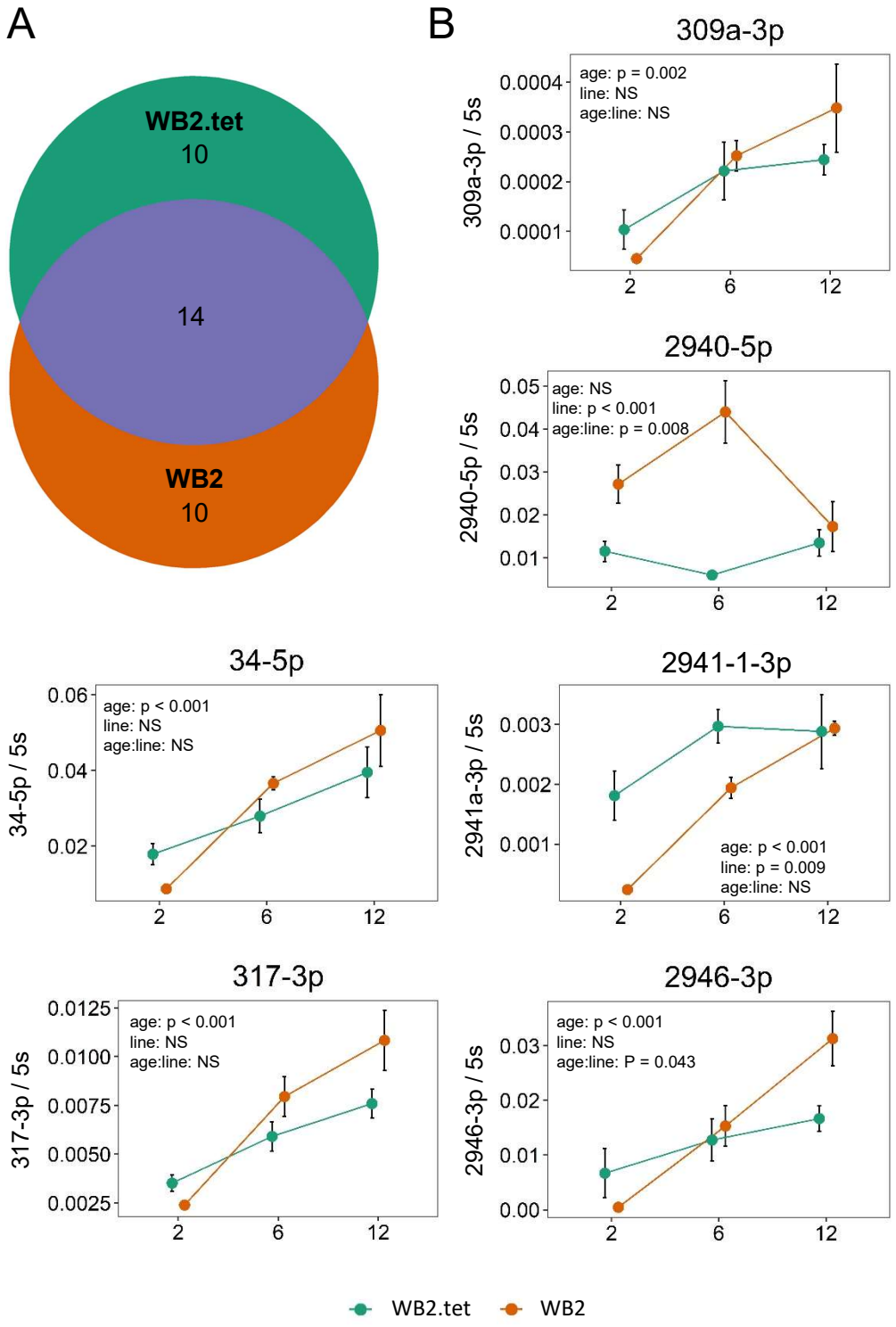
A
WB2.tet
10
14
WB2
10
B
309a-3p
309a-3p / 5s
0.0004
0.0003
0.0002
0.0001
age: p = 0.002
line: NS
age:line: NS
2
6
12
2940-5p
2940-5p / 5s
0.05
0.04
0.03
0.02
0.01
age: NS
line: p < 0.001
age:line: p = 0.008
34-5p
34-5p / 5s
0.06
0.04
0.02
age: p < 0.001
line: NS
age:line: NS
2941-1-3p
2941a-3p / 5s
0.003
0.002
0.001
age: p < 0.001
line: p = 0.009
age:line: NS
317-3p
317-3p / 5s
0.0125
0.0100
0.0075
0.0050
0.0025
age: p < 0.001
line: NS
age:line: NS
2946-3p
2946-3p / 5s
0.03
0.02
0.01
0.00
age: p < 0.001
line: NS
age:line: P = 0.043
WB2.tet
WB2

Fig. 6

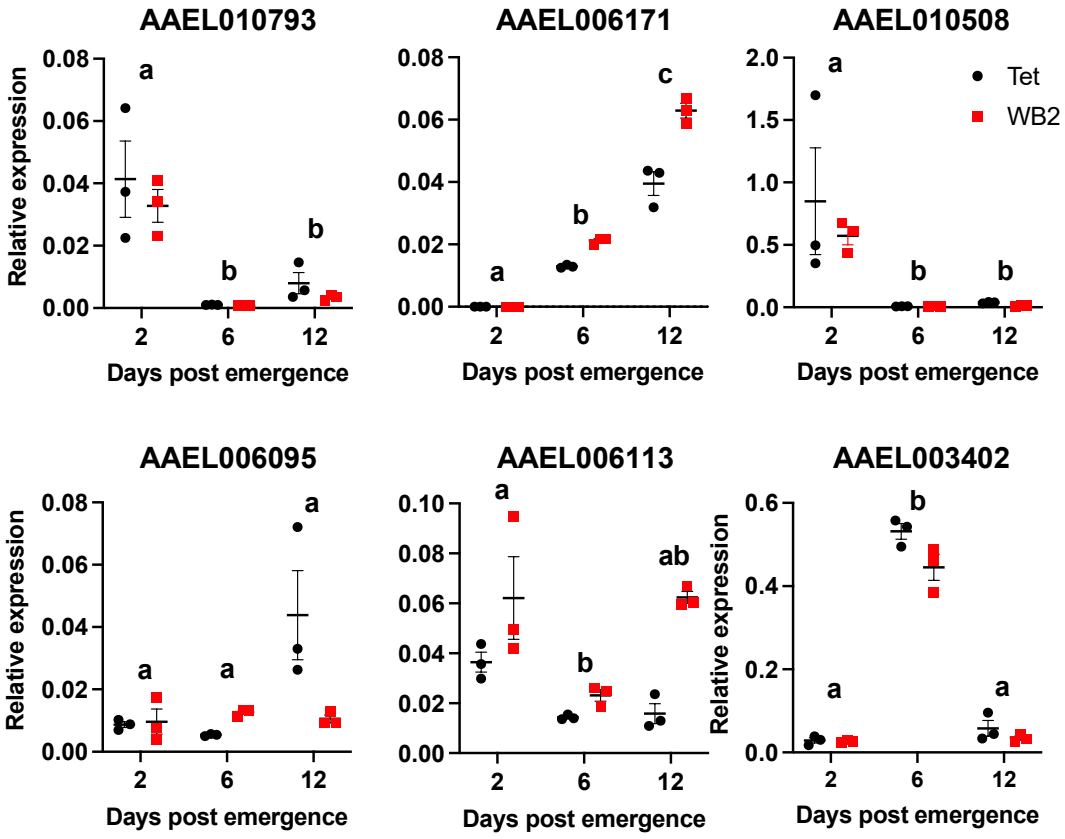
AAEL010793
AAEL006171
AAEL010508
AAEL006095
AAEL006113
AAEL003402
Relative expression
Days post emergence
Tet
WB2
a
b
c
ab
0.08
0.06
0.04
0.02
0.00
0.10
2.0
1.5
1.0
0.5
0.0
0.6
0.4
0.2
2
6
12

Fig. 7

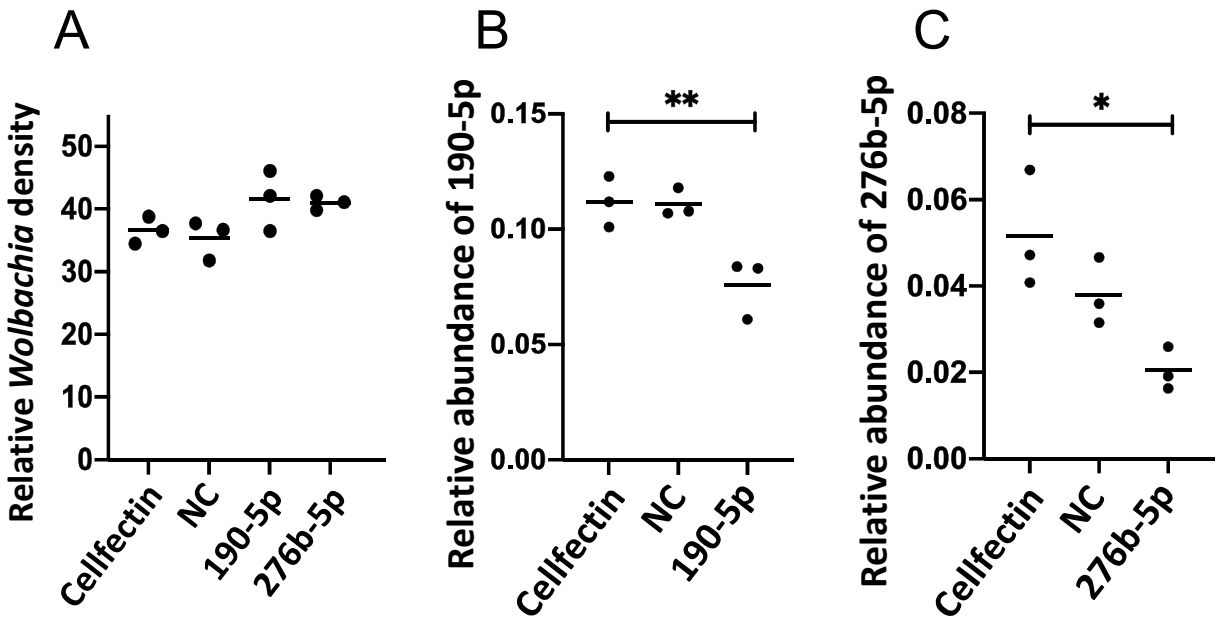
A
Relative *Wolbachia* density
50
40
30
20
10
0
Cellfectin
NC
190-5p
276b-5p
B
Relative abundance of 190-5p
0.15
0.10
0.05
0.00
**
Cellfectin
NC
190-5p
C
Relative abundance of 276b-5p
0.08
0.06
0.04
0.02
0.00
*
Cellfectin
NC
276b-5p

Fig. 8

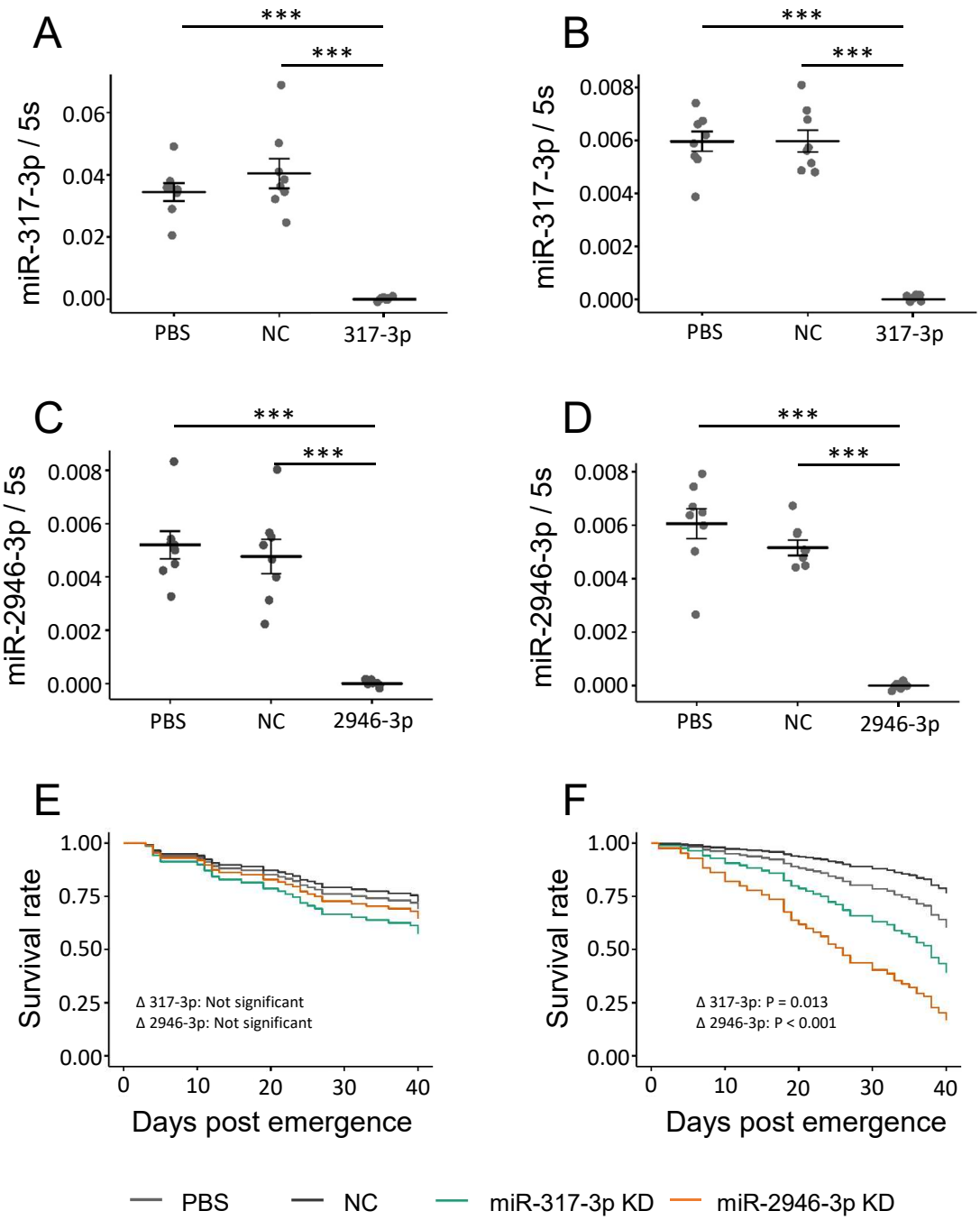
A
***
***
miR-317-3p / 5s
0.06
0.04
0.02
0.00
PBS
NC
317-3p
B
***
***
miR-317-3p / 5s
0.008
0.006
0.004
0.002
0.000
PBS
NC
317-3p
C
***
***
miR-2946-3p / 5s
0.008
0.006
0.004
0.002
0.000
PBS
NC
2946-3p
D
***
***
miR-2946-3p / 5s
0.008
0.006
0.004
0.002
0.000
PBS
NC
2946-3p
E
Survival rate
1.00
0.75
0.50
0.25
0.00
Δ 317-3p: Not significant
Δ 2946-3p: Not significant
0
10
20
30
40
Days post emergence
F
Survival rate
1.00
0.75
0.50
0.25
0.00
Δ 317-3p: P = 0.013
Δ 2946-3p: P < 0.001
0
10
20
30
40
Days post emergence
PBS
NC
miR-317-3p KD
miR-2946-3p KD